Journal of Sound and Vibration 450 (2019) 175–198

Contents lists available at ScienceDirect

Journal of Sound and Vibration

journal homepage: www.elsevier.com/locate/jsvi

Aeroacoustics research in Europe: The CEAS-ASC report on 2017 highlights

Lars Enghardt

German Aerospace Center (DLR), Müller-Breslau-Str. 8, 10623, Berlin, Germany

ARTICLE INFO

Article history:
Received 31 January 2019
Revised 1 March 2019
Accepted 6 March 2019
Available online 14 March 2019
Handling Editor: J. Astley

ABSTRACT

The Council of European Aerospace Societies (CEAS) Aeroacoustics Specialists Committee (ASC) supports and promotes the interests of the scientific and industrial aeroacoustics community on the European scale, and European aeronautics activities internationally. Each year, the committee highlights several of the research and development projects in Europe. This paper is the 2017 issue of this collection of Aeroacoustic Highlights, compiled from contributions submitted to the CEAS-ASC. The contributions are classified under five main headings: Airframe Noise, Jet Noise, Turbomachinery Noise, Techniques and Methods in Aeroacoustics and Further Applications of Aeroacoustics. A concise summary of the CEAS-ASC workshop held in Dublin, Ireland, in September 2017 is also included in this report.

1. Introduction

The CEAS-ASC each year provides a report summarizing significant advances in aeroacoustic research fields. The present paper corresponds to the 2017 edition of this report. As for previous editions, it would be impossible to give a detailed view of the scientific activity in each research topic, and the present paper focuses on innovative advances and findings from accomplished projects funded by European, industrial or national programmes. The paper is organised as a collection of contributions, divided into sections corresponding to the main topics of research in 2017.

2. CEAS-ASC workshop

The 21st Scientific Workshop of the Aeroacoustics Specialists Committee of the CEAS was hosted by the School of Engineering in Trinity College Dublin, the University of Dublin, on September 13–15, 2017. The topic was *Aircraft Noise Generated from Ducted or Un-Ducted Rotors*. It was organised by Assoc. Prof. Gareth J. Bennett who was also the Chair of the Scientific Committee. The workshop focused on rotor noise in the domain of aviation, including sources related to the installation of rotors on aircraft. Research activity detailing developments in un-ducted propulsion systems such as CROR/Turbo-Prop/Unducted Single Fan (USF) etc. were welcome. In addition, the scope of the workshop included ducted rotor noise originating in turbomachinery or compressors. The presentations were delivered in five sessions entitled: Developments in Analytical Methods; Results and Analysis from Measurement Campaigns; Novel Measurement Methods; Modelling and Computational Analysis Providing Novel Insight; Sound Generation Through Rotor Installation and Related Inflow Inhomogeneity. The Scientific Workshop is typically a small but high-level scientific meeting of a single track and with sufficient time allocated to allow for discussion, sharing insight and for identifying future opportunities. This meeting attracted a lot of interest in 2017 with 31 scientific presentations delivered

E-mail address: Lars.enghardt@dlr.de.

https://doi.org/10.1016/j.jsv.2019.03.006
0022-460X/

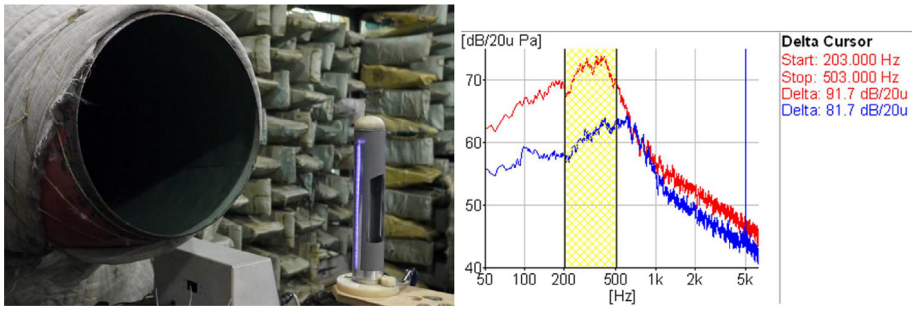

Fig. 1. Left: A photo of a cylinder with plasma actuators in the cross-flow. Right: Far-field SPL spectra for flow velocity 80 m/s. Red curve: actuator off, blue curve: actuator on, actuation frequency F = 5 kHz. (For interpretation of the references to colour in this figure legend, the reader is referred to the Web version of this article.)

with 29 individual institutions represented from all over the EU and from as far afield as Canada, the US, Israel and the Russian Federation. Four keynote talks were delivered by: Prof. Dr. Lars Enghardt, DLR, *Recent Fan Broadband Noise Activities within the Framework of European* Funded *Collaborative Research Projects*; Dr. Kevin Britchford, Rolls-Royce, UK, *Future Noise Challenges from Gas Turbine Engine Compressors and Turbines*; Prof. Dr. Scott Morris, University of Notre Dame, *A Discussion of Broadband Rotor Noise* and by Dr. David Stephens, NASA Glenn, *Fan Noise and Inflow Distortion*. Acknowledgement is extended to AIRBUS for sponsoring the workshop and for their generous financial contribution as well as to Fáilte Ireland and the AIAA as secondary sponsors. Further detail of the 2017 workshop in Trinity College Dublin, as well as the full proceedings, can be found at http://bit.ly/CEAS-ASC-2017. The research activity presented at the workshop was of an exceptionally high standard and a special issue in the International Journal of Aeroacoustics was published based on a selection of papers from the workshop [1–5]. The issue included analytical, numerical and experimental work and encompasses the full breadth of research activity in this topical area.

Submitted by Gareth J. Bennett, gareth.bennett@tcd.ie*, Technical Chair CEAS-ASC Workshop 2017, University of Dublin, School of Engineering in Trinity College Dublin.*

3. Airframe noise

3.1. Cylinder noise reduction with plasma actuators

Reduction of aerodynamic noise due to flow around a cylinder is an important problem, relevant to development of methods for airframe noise mitigation. Plasma actuators are known to reduce airframe noise in low-speed flows, where incoming flow velocity is comparable to flow velocity induced by the actuators (about 10 m/s). To study the control authority of plasma actuators over aerodynamic noise of a cylinder in higher-speed flows, parametric tests in an anechoic chamber were carried out for surface high frequency dielectric barrier discharge (HF DBD) plasma actuators (Fig. 1, left). Experiments were performed for incoming flow velocities up to 80 m/s (Reynolds number 2.2×10^5), which corresponds to aircraft speed at landing, and demonstrated that HF DBD actuators can considerably reduce aerodynamic noise of a cylinder for these velocities as well. As flow velocity increases, the value of noise reduction in the frequency range of spectral maximum increases from 5 dB (for 40 m/s) to 10 dB (for 80 m/s, see Fig. 1, right). This value is also sensitive to the position of the electrodes on the cylinder surface. PIV measurements demonstrated that noise reduction is accompanied by significant reorganization of the wake behind the cylinder, decreasing both wake width and turbulence level. The experiments seem to corroborate the conclusion that the main mechanism of HF DBD actuator effect on flow around a cylinder and on radiated noise is due to gas heating by the discharge. Since HF DBD plasma actuators are shown to have the control authority over cylinder noise for flow velocities of technological interest, these actuators may be considered as a candidate for aircraft landing gear noise reduction. This work was supported by a grant of the Russian Ministry of Education and Science, no. 14.Z50.31.0032.

Submitted by Victor Kopiev, vkopiev@mktsagi.ru*, Central Aerohydrodynamic Institute (TsAGI), PNIPU, Moscow, Russia.*

3.2. Airframe and engine noise emission model for time-step simulation programs

Airframe noise of turbofan powered aircraft is the dominating sound source for large parts of the approach procedure. Still, many best practice aircraft noise calculation models neglect the influence of airspeed and aeroplane configuration. To describe airframe noise independently from engine noise emissions, two separate multiple linear regression models were developed with the help of physical principles, data exploration, and engineering judgement [6]. Aircraft noise measurements and flight data records from real air traffic served as data basis to establish the spectral model coefficients for several commercial aircraft. The airframe noise model accounts for a two-dimensional directivity, the aircraft Mach number, air density and aeroplane configuration. Fig. 2(left) shows how the overall sound emission level L_{em} (unweighted, directional sound power, details see Ref. [6]) changes with the use of speedbrakes and landing gear in function of the Mach number. The engine

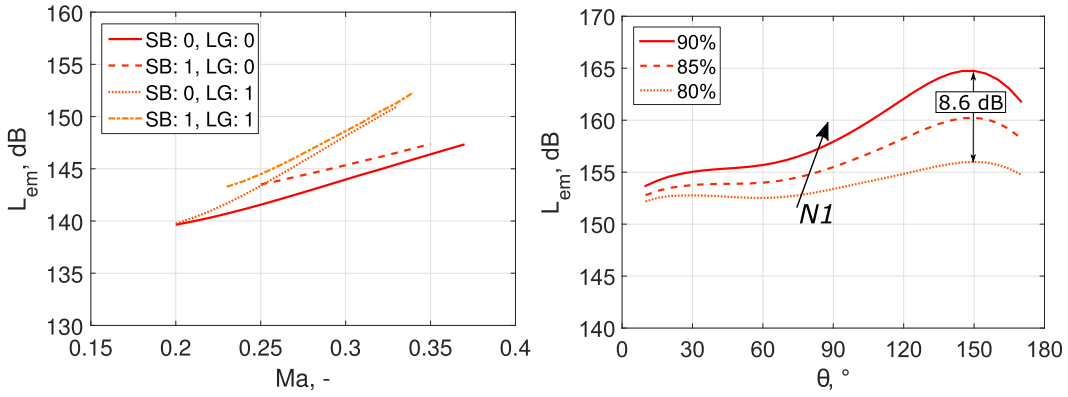

Fig. 2. Left: Relationship of the overall sound emission level (L_{em}) to the polar angle θ for different N1-values at take-off for the A333 (Trent 700). Predicted with Ma = 0.26, ρ = 1.15 kg/m^3. Right: Relationship of the overall sound emission level (L_{em}) to the Mach number for different aeroplane configurations (SB: speedbrakes, LG: landing gear) at approach for the A333 (Trent 700). Predicted with N1 = 30%, ρ = 1.1 kg/m^3.

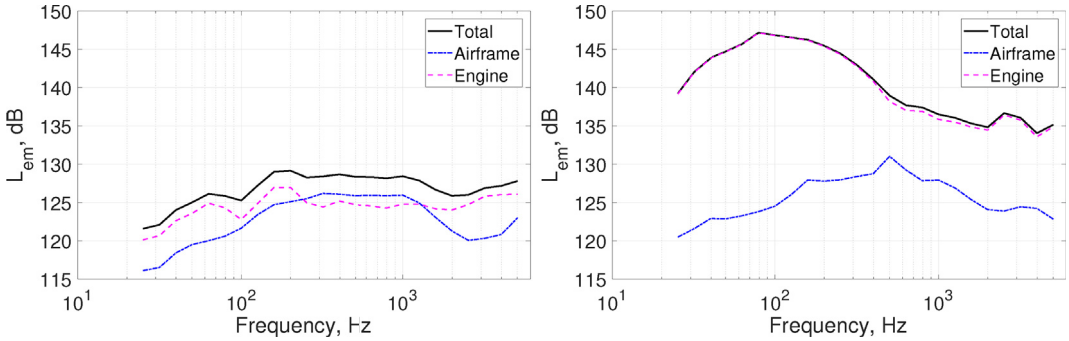

Fig. 3. Left: Noise emission spectra at the rear of the A320 (CFM56-5B) for final approach (θ = 130°, N1 = 55%, Ma = 0.23). Right: Noise emission spectra at the rear of the A320 (CFM56-5B) for take-off (θ = 130°, N1 = 93%, Ma = 0.24).

noise model accounts for a three-dimensional directivity, the rotational speed of the fan shaft (N1 in %), and the Mach number. Fig. 2(right) depicts the influence of N1 on sound emission as a function of the polar angle for typical N1-values at take-off. The directivity pattern changes with increasing N1 due to jet and fan noise. Fig. 3 presents spectra of airframe and engine noise for typical flight configurations (final approach and take-off) and their varying share on the total sound emission spectrum. More details on the model development and its verification can be found in Ref. [7]. The models will be applied to the assessment and optimization of noise abatement procedures, e.g., by using flight parameters from full-flight simulators. Such studies can be conducted with the simulation program sonAIR [8], which combines aircraft noise emission and sound propagation in a time-step simulation procedure to calculate noise exposure maps of single flight as well as complex scenarios.

Submitted by Christoph Zellmann, christoph.zellmann@empa.ch, J.M. Wunderli, B. Schäffer, EMPA, Switzerland, and U. Isermann, DLR, Germany.

4. Jet noise

4.1. Numerical analysis of the impact of the interior nozzle geometry on low Mach number jet acoustics

Real nozzle configurations often contain internally mixed multi-shear-layer flows such that the multiple jet streams influence the noise level in the near field quite dramatically. For the three nozzle shapes shown in Fig. 1., the numerical analysis based on the hybrid large-eddy simulation (LES)/acoustic perturbation equations (APE) approach concentrates on the effect of the geometric details inside the nozzle on the flow field and the acoustic field [9]. Besides the clean nozzle, one nozzle configuration contains a centerbody and another configuration consists of a centerbody plus struts such that compared to a clean configuration without any built-in components additional shear layers and wakes are generated whose effects on the acoustic field were investigated. The LES method is based on hierarchically refined Cartesian meshes, where the nozzle wall boundaries are resolved by a conservative cut-cell method. The APE solution is determined on a b lock structured mesh. The differences of the sideline acoustics are illustrated in Fig. 4. The acoustic radiation perpendicular to the jet axis (side-

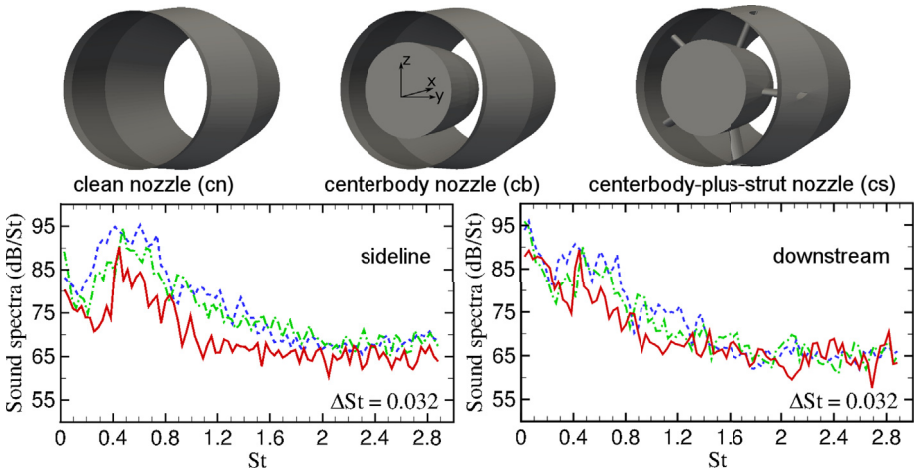

Fig. 4. Power spectra of the acoustic pressure signals determined for the three nozzle geometries cn (solid line), cb (dashes), and cs (dash-dot) in a sideline and a downstream position.

line) is clearly intensified for the centerbody configurations cb and cs than that of the cn configuration. The detailed analysis showed an important dependence of the jet acoustic near field on the presence of the nozzle built-in components. The centerbody generated a rather broad hump in the acoustic spectra. The azimuthally correlated large scale coherent structures shed from the centerbody generated this broad region which is partly removed by the enhanced turbulent mixing excited by the struts.

Submitted by Seong Ryong Koh, O. Cetin, M. Meinke, W. Schröder, s.koh@aia.rwth-aachen.de*, Institute of Aerodynamics, RWTH Aachen University, Germany.*

4.2. Turbulent jet simulations using high-order DG methods for aeroacoustics analysis

Despite recent progress ([10–13]), accurately simulating a turbulent jet remains a challenge. Strategies have indeed been developed to trigger the transition to turbulence within the nozzle. However, a fine resolution is still needed to convect the turbulent fluctuations.

Discontinuous Galerkin (DG) methods ([14,15]) appear as an interesting approach to capture the complex physics involved in turbulent jet flows, as they provide high-order of accuracy on unstructured meshes, as well as excellent parallel capabilities.

This work aims at providing a first evaluation of the high-order DG approach for aeroacoustic simulations of turbulent jets (ref [7]). A fourth-order modal DG method is used to perform an LES of a turbulent jet at Reynolds number $Re = 10^6$ and $M = 0.9$. The far-field noise is evaluated using the Ffowcs Williams and Hawkings surface integral formulation. The numerical results are compared to a reference second-order FV LES ([16]) and to experimental data. Both LES are performed on fully unstructured grids using the Smagorinsky model.

At this stage, no boundary layer forcing technique is yet used. This is left for future work. As a consequence, both simulations present a laminar shear layer at the nozzle exit. The DG simulation presents however a transition to turbulence slightly closer to the nozzle exit (Fig. 5(left)). This is related to the broader frequency band resolved (both in time and space) in this region thanks to the greater accuracy provided by the DG method. This in turn leads to a lower jet spreading rate which explains the discrepancies found with the experimental results (Fig. 5(right)). As regards the far-field acoustic field, an overall good match is obtained, see Fig. 6.

These results demonstrate the capacity of the high-order DG method to perform aeroacoustic analyses of turbulent jets. Future work will deal with the use of turbulence triggering as well as hp-adaptation techniques and the Variational Multiscale approach to LES ([17]).

Submitted by Mathieu Lorteau, mathieu.lorteau@onera.fr*, Marta de la Llave Plata, Vincent Couaillier, François Vuillot and Nicolas Lupoglazoff, ONERA, France.*

4.3. Identification of hydrodynamic and acoustic nature of the pressure POD modes in the near field of a subsonic jet

The use of Proper Orthogonal Decomposition (POD) is a powerful tool to reveal the jet structure, but its interpretation is usually not trivial. Indeed, the mere existence of POD modes does not imply their dynamical significance in terms of noise generating flow. The discussion above motivated the work conducted by Ref. [19], where a physical criterion for the interpretation of the near-field pressure POD modes in terms of hydrodynamic and acoustic pressures was provided. An experimental test campaign [20,21] involving simultaneous near- and far-field pressure measurements on a subsonic jet for M_j was carried out

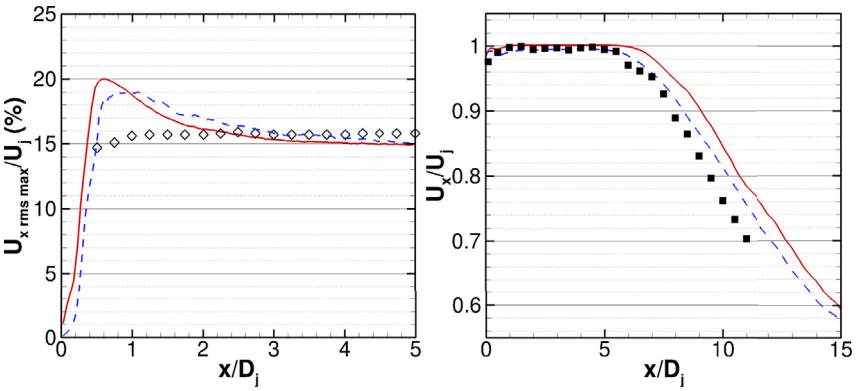

Fig. 5. Left: Comparison of the longitudinal evolution of $U_{xrmsmax}$. Solid red: DG, dashed blue: FV, symbols: taken from Ref. [18]. Right: Comparison of the axial evolution on the jet axis of the mean axial velocity. Solid red: DG, dashed blue: FV, symbols: measurements. (For interpretation of the references to colour in this figure legend, the reader is referred to the Web version of this article.)

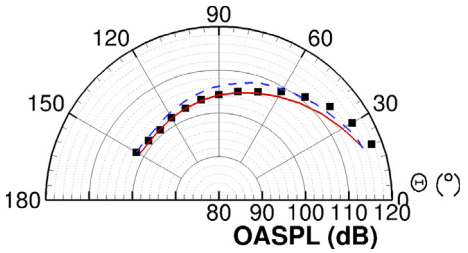

Fig. 6. OASPL of the pressure field in the far field at 30D from the nozzle exit. Solid red: DG, dashed blue: FV, symbols: measurements. (For interpretation of the references to colour in this figure legend, the reader is referred to the Web version of this article.)

at the École Centrale de Lyon. The streamwise structure of the near-field pressure was provided by POD. The wavenumber-frequency spectrum of the re-constructed pressure fields using each POD mode was computed. The hydrodynamic/acoustic nature of the POD modes was assessed based on the location of the spectral energy peak in the $k_x - \omega$ domain. According to the scheme depicted in Fig. 7, hydrodynamic, acoustic and hybrid hydro-acoustic modes are detected on account of the phase velocity of the spectrum peaks. Three types of hybrid modes were detected based on the topology of the $k_x - \omega$ spectrum. The representation of the $k_x - \omega$ spectra for all the different types of modes is shown in Fig. 8. It is observed that the acoustic mode and the acoustic content of the hybrid 3 mode are characterised by a phase speed tending to infinity, thus indicating acoustic waves propagating in the sideline direction in the far field. Whereas the acoustic content of the hybrid modes 1–2 is characterised by a phase speed of the order of the speed of sound, thus suggesting a downstream preferential propagation direction in the far field. Such assertions are supported by computing the cross-correlation with the measured far-field noise, as shown in Fig. 9.

Submitted by Matteo Mancinelli, matteo.mancinelli@univ-poitiers.fr, Institut Pprime - CNRS, Université de Poitiers, ENSMA - Département Fluides, Thermique et Combustion, Chasseneuil, Poitiers, France, Tiziano Pagliaroli, Università Niccolò Cusano, Dipartimento di Ingegneria, Roma, Italy, Roberto Camussi, Università degli Studi Roma Tre, Dipartimento di Ingegneria, Italy, Thomas Castelain, Claude Bernard University Lyon 1, Laboratoire de Mécanique des Fluides et Acoustique, France.

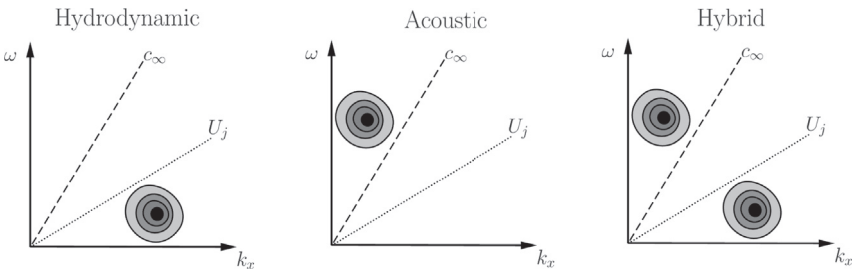

Fig. 7. Scheme of interpretation of the POD modes based on the location of the spectral energy location in the wavenumber-frequency domain.

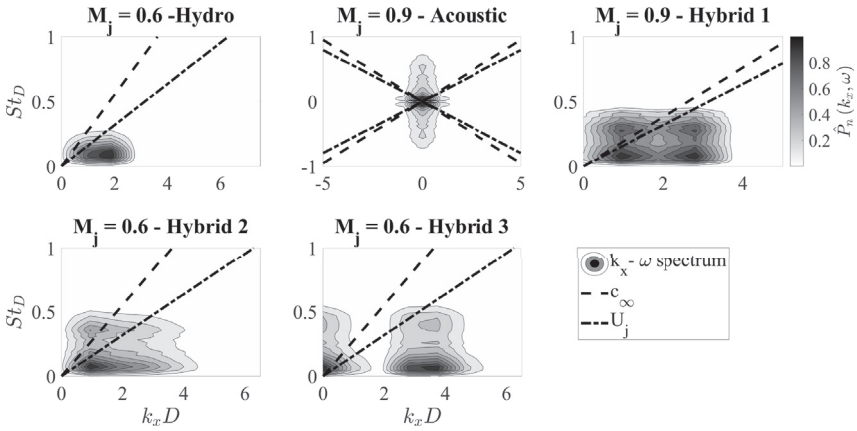

Fig. 8. Identification of the nature of the POD modes through the wavenumber-frequency spectrum of the re-constructed near pressure fields for both jet Mach numbers.

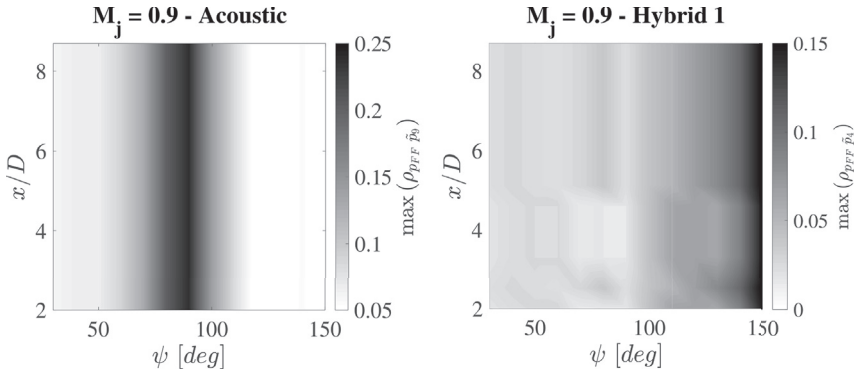

Fig. 9. Example of the cross-correlation coefficient maps between the far-field and the re-constructed near-field pressures by using acoustic and hybrid type 1 POD modes.

4.4. Crackle and screech noise generated by laboratory scale cold supersonic jets

Supersonic jet noise has several components mixing noise that includes Mach waves and crackle, broadband shock associated noise and screech noise that occur only in non-ideally expanded jets. Although crackle noise can account for about a third of the acoustic power emitted from a supersonic jet of $M_J = 2$, it is probably the least investigated. This is because of the difficulties in capturing its spectral signature. It is known to be composed of low frequency random noise of steepening waves at the quadrant of the Mach direction. Hence measures based on skewness can be used to identify it. However, some controversy exists about the source of this noise, the skewness of the pressure derivative, dp/dt rather than pressure p.

An experimental study of crackle and screech generated by a cold under-expanded supersonic jet of $M_J = 2$ of lab size was recently published [22]. The ratio of the reservoir to ambient pressure was 1.35 and crackle was found in the far field of the Mach direction quadrant. A harmonic screech tone was also found sideways to the jet. Both crackle and screech showed high level of skewness of about 0.65 in p, but crackle also showed high skewness in dp/dt of about 0.7 while only 0.2 for screech. It was shown earlier in Ref. [22] that in the near field both signals were Gaussian and thus high skewness in the farfield was associated with nonlinear propagation and 'bunching' process caused shift towards low frequency.

Measurements for an over-expanded jet of reservoir to ambient pressure ratio of 0.3 showed reduced crackle noise. This was associated with the reduced low frequency noise component and reservoir pressure. However, screech was still found, including a fundamental tone at the Mach direction quadrant of 400 as shown in Fig. 10. Skewness measurement confirmed a reduced level of crackle.

Submitted by Jyothi Punekar, jyothi.punekar@gmail.com, and Eldad Avital, Queen Mary University of London, London, United Kingdom.

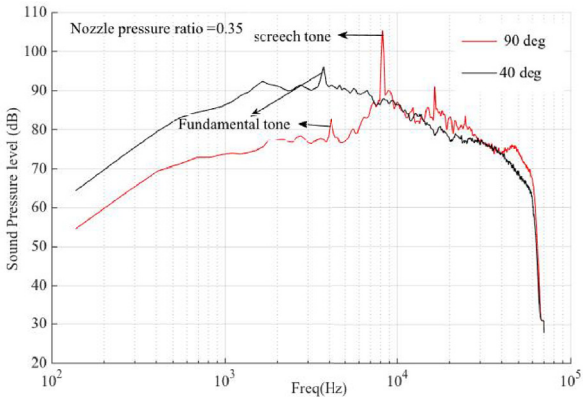

Fig. 10. Spectral contents of far-field over expanded jet at 40d and 90° respectively.

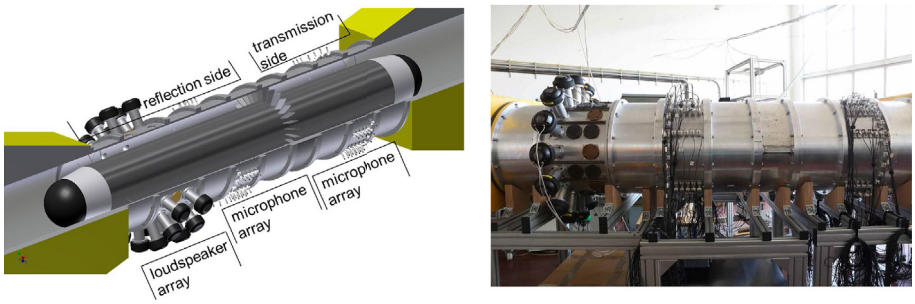

Fig. 11. Experimental setup for the investigation of mode transmission through stator vane rows.

5. Turbomachinery Noise

5.1. Comprehensive experimental investigation of mode transmission through stator vane rows

The mode transmission through turbomachinery stages is an important aspect for the prediction of the sound radiation from aero-engines and its constituents such as multi-stage low pressure turbines. In an experimental investigation a comprehensive database of the mode transmission through stator vane rows was established [23]. It comprises a wide variation of the stator vane geometry, starting from simple flat plate cascades to cambered airfoil geometries. In total 27 configurations were investigated. The experimental setup (Fig. 11) consisted of a loudspeaker array and optimized microphone arrays on each side of the stator vane row. A new method was developed, which allows performing the investigation using reduced sensor arrays, i.e. the modal sound field is subsampled. Therefore, the radial mode analysis was extended to the concept of Compressed Sensing [24]. The determination of the complete scattering matrix and in particular the transmission and reflection factors is performed on the set of measured transfer functions between each loudspeaker and microphone.

The results for flat plate cascades were compared regarding different stagger angles and vane count. Differences to an analytical 2D cascade model [25], which is based on the model of Smith [26], were highlighted. The experimental results are used to calibrate the analytical cascade model, by removing the singular behavior for no flow conditions. The calibrated model achieves a good agreement for the reconstruction of experimental results for the flat plate configurations (Fig. 12) and is capable of predicting the mode transmission and reflection of vane rows with complex airfoil geometries.

Further, the experimental database will be used to validate analytical prediction tools and numerical codes and identify possible means for further development in order to improve the pre-design capabilities for turbomachinery components.

Submitted by Maximilian Behn, maximilian.behn@dlr.de, L. Klähn and U. Tapken, German Aerospace Center (DLR), Germany.

5.2. Fan broadband noise predictions

After previous successful applications of the flow solver PowerFLOW to airframe noise generation and radiations problems [27–29], the 22-in Source Diagnostic Test (SDT) fan/outlet guide vane (OGV) experiment of NASA Glenn Research Center was reproduced numerically using the same lattice-Boltzmann/very large-eddy technology [30]. Three OGV configurations and one rotational speed were considered, corresponding to an approach flight condition. Comparisons with available measurements of

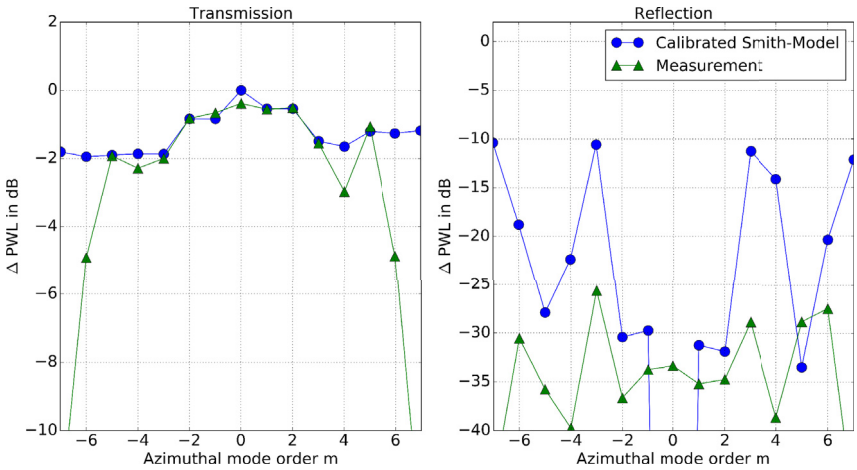

Fig. 12. Transmission and reflection losses for a cascade with 15 flat plates, chord length of 96 mm and a stagger angle of 0°. The measurement is shown as green triangles and the reproduced results using the calibrated analytical model as blue dots. (For interpretation of the references to colour in this figure legend, the reader is referred to the Web version of this article.)

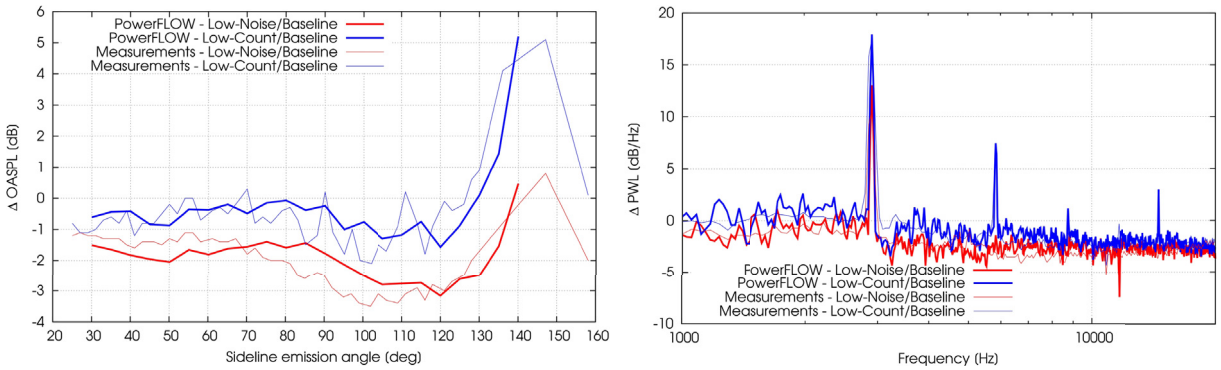

Fig. 13. SDT fan stage, approach condition (7809 rpm), low-noise and low-count configuration, measurements vs. predictions: Relative far-field OASPL along the sideline array (left) and relative PWL (right).

the noise power level (PWL) and far-field overall sound pressure level (OASPL) revealed consistent trends between the three OGV configurations. In particular, the predicted PWL (Fig. 13(left)) and OASPL (Fig. 13(right)) differences between the baseline and the other OGVs were found in less than 1 dB agreement with the measurements. A time/circumferential Fourier analysis of the computed field revealed the broadband nature in time and space of the acoustic field, thus motiva ting the usage of time-domain solutions for nacelle and liner design and optimizations. The computational turnaround time was in the order of one week per design on a 720-core cluster, which is compatible with the development time of a new engine. Finally, the feasibility of simulations including a honeycomb liner was investigated as an alternative to the usage of a wall impedance model.

Submitted by Damiano Casalino, damiano@exa.com, Exa GmbH, Stuttgart, Germany.

5.3. A thin active acoustic liner aiming at reducing the low-frequency tonal noise of UHBR architectures

The main technology of acoustic treatments currently used on turbofan engines is the acoustic liner, formed of a distribution of small cavities in a honeycomb structure glued between a perforated facing sheet and a reflective, solid backing sheet. As they are intrinsically resonant (quarter-wavelength resonators), their efficiency is limited frequency-wise due to their size. However, future UHBR engine technologies with fans of larger dimensions are expected to produce tonal noises shifted towards the low frequencies, while presenting less surface and thickness for acoustic treatments, thus requiring new technologies of acoustic liners with subwavelength sound absorption. Within the frame of the FP7-funded project ENOVAL (grant agreement n° 604999), an active sound absorption technology has been developed for use in a novel active acoustic liner concept, aiming at breaking the quarter-wavelength rule [31]. This task was led by a pool of universities (Ecole Polytechnique Fédérale de Lausanne, FEMTO-ST Institute in Besançon, and Ecole Centrale de Lyon) under the supervision of Safran-Nacelles. The technology, based on the Electroacoustic Absorber concept developed at EPFL [32], relies on the use of conventional electrodynamic

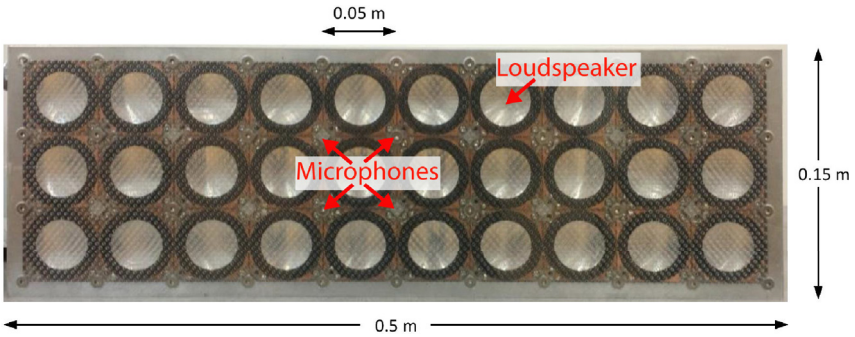

Fig. 14. Front view of the developed prototypes composed of 3 × 10 small Electroacoustic Absorbers.

loudspeakers, down-scaled for aircraft applications, one or more microphones, and an individual electronic controller feeding the loudspeaker through a voltage-driven current amplifier. With such control architecture, it is possible to design either Single Degree-Of-Freedom or Multiple Degrees-Of-Freedom resonators, resulting in either narrow-band or broadband sound absorbers. In the SDOF case, it is possible to completely discard the passive resonant behavior of the passive membrane of the loudspeaker (passive SDOF with natural resonance frequency fn and acoustic resistance rn), and tweak it to present a target acoustic resistances rt, while shifting its resonance frequency to a target value ft. The latter strategy was then chosen to design adjustable SDOF with different central frequencies, leading to the development of a prototype made of 3 × 10 unit-cells (overall size 50 cm × 15 cm x 8 cm, see Fig. 14). The liner prototype is composed of small electrodynamic loudspeakers (diameter 5 cm and thickness 2.5 cm), surrounded by 4 tiny microphones, and controlled through an individual microcontroller and current amplifier, the whole being commanded by a centralized interface through a multilayer electronic board assembly (additional thickness of 5.5 cm).

The prototype was then installed in the NLR Acoustic Flow Duct Facility for the assessment of the achieved Insertion Losses with the different control settings and different flow conditions (however limited to M = 0.15 due to the control microphone dynamics limitations). These ILs (see Fig. 15(above) without flow and Fig. 15(below) with M = 0.15) present the highest value of 16 dB when the Electroacoustic Absorbers are controlled with ft = fn and $rt = \rho^* c/2$. It has also been possible to adjust the resonance frequency from around fn/2 up to almost 2 fn, with degraded ILs as ft moves away from fn (without flow: IL = 6 dB when ft = fn/2, IL = 16 dB at ft = fn, and IL = 10 dB at ft = 1.25 fn with M = 0.15: IL = 16 dB at ft = fn and IL = 5 dB at ft = 1.75 fn) [33].

Submitted by Hervé Lissek, herve.lissek@epfl.ch, Ecole Polytechnique Fédérale de Lausanne, Switzerland.

5.4. Broadband noise prediction of a low-noise serrated OGV using 3D CAA with synthetic turbulence approach

Leading edge treatments based on sinusoidal serrations aimed at reducing turbofan interaction noise have been extensively investigated in Europe through numerous studies, focusing on isolated airfoil interacting with a homogeneous turbulence [34]. Onera has investigated a 3D numerical simulation of such treatment in (Fig. 16) a rotor-stator configuration using a time-domain Euler solver with a synthetic turbulence model. This simulation is coupled to a Ffowcs-Williams and Hawkings integral tailored to induct noise propagation. The computational methodology was validated by comparison with experimental data from NASA SDT test-case [35]. As a first application, a SAFRAN Aircraft Engines turbofan model with reference and serrated OGV's have been simulated and the expected noise reduction restricted up to now to academic turbulence-airfoil cases has been numerically highlighted and generalized here to an industrial fan stage configuration. RANS solutions providing turbulent wake characteristics are used to adjust the serration design. This design has been constrained with respect to aerodynamic performances of the rotor-stator stage, so that pressure losses and isentropic efficiency were found acceptable, and a high regime not too far from the ADP (Aerodynamic Design Point) has been considered. Hence, the predicted OAPWL reduction is almost 2 dB with a maximum of 4 dB at higher frequencies, but higher overall level attenuation should be expected for lower speed regimes (typically at approach condition) (see Fig. 17).

Submitted by Gabriel Reboul, gabriel.reboul@onera.fr, A. Cader, C. Polacsek, T. Le Garrec and R. Barrier, ONERA - The French Aerospace Lab., France.

5.5. Back to back aeroacoustic test of a turbine exhaust case with and without acoustic treatment

Within the EU FP7 project ENOVAL (grant agreement n° 604999) a back to back aeroacoustic test of a turbine exhaust case (TEC) with and without acoustic treatment was carried out in cooperation between MTU Aero Engines, GKN Aerospace and DLR. The test object is a state of the art, full scale, three stage low pressure turbine run at an operating point relevant for acoustic certification. The objective of the acoustic tests is the detailed assessment of the impact of the acoustic liners on the radiated sound power of the turbine. For the back to back test one configuration has liners installed in the passages between

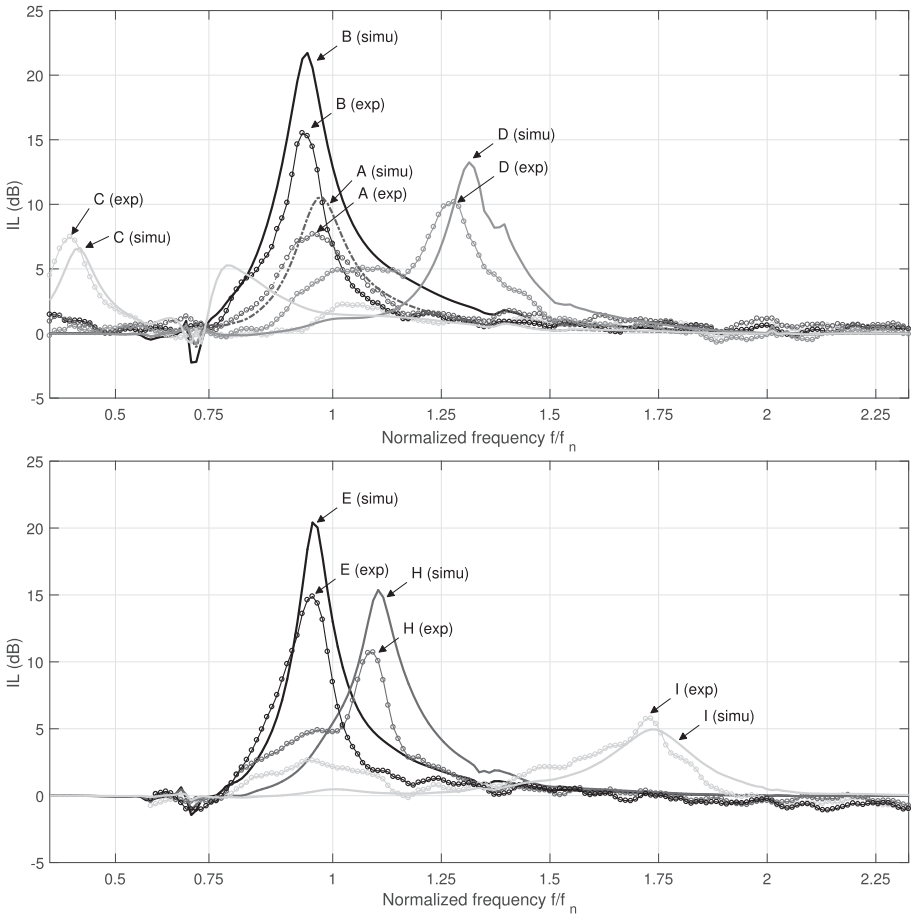

Fig. 15. Above: IL obtained without flow. The different curves present the simulated (marked curves) and measured (plain curves) results of different control cases (labelled A, B, C and D). Below: IL obtained with M = 0.15. The different curves present the simulated (marked curves) and measured (plain curves) results of different control cases (labelled AE, H and I).

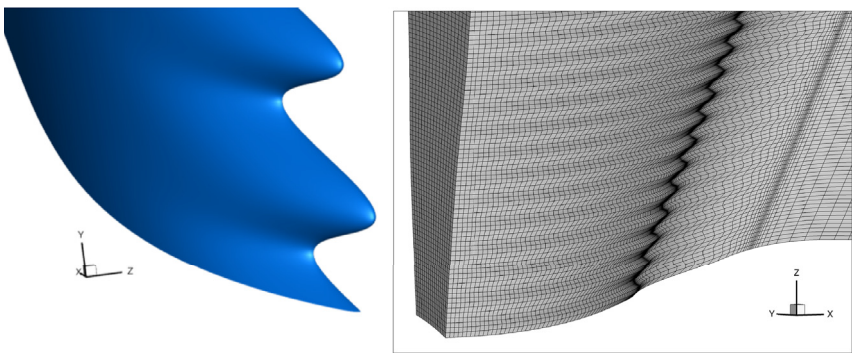

Fig. 16. 3D views of serrated OGV geometry (left) and 1-vane channel CAA grid (right).

the TEC vanes at the hub and at the shroud. The other configuration has acoustically hard walls. The turbine and TEC design has been created in collaboration between MTU and GKN for reduced length, increased performance and reduced noise. In a straight annular section downstream of the TEC a microphone array, which has been designed by DLR, is used to acquire the acoustic pressure. The pressure distribution is depicted in Fig. 18 for one of the blade passing frequency (BPF) components of the turbine. The microphone array consists of 120 Microphones installed wall flush at the hub and at the shroud. It can be traversed circumferentially to form a regular grid of 7200 measurement positions. On this fine grid the inverse radial mode analysis technique described by Tapken [36] is used to perform a modal breakdown of the BPF tones and to calculate the sound

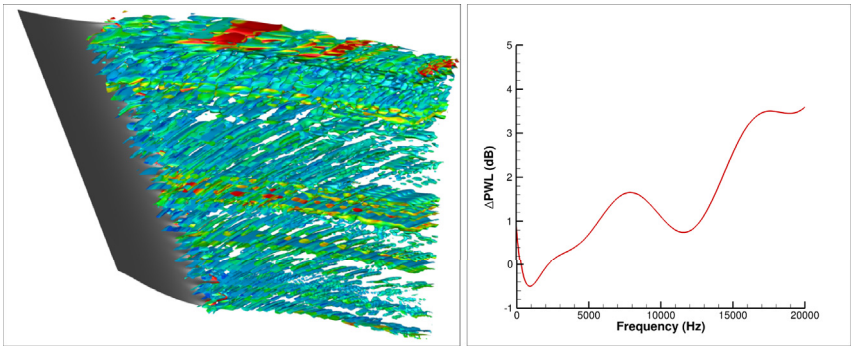

Fig. 17. Left: Synthetic turbulent vorticity field. Right: Delta PWL reduction issued from CAA.

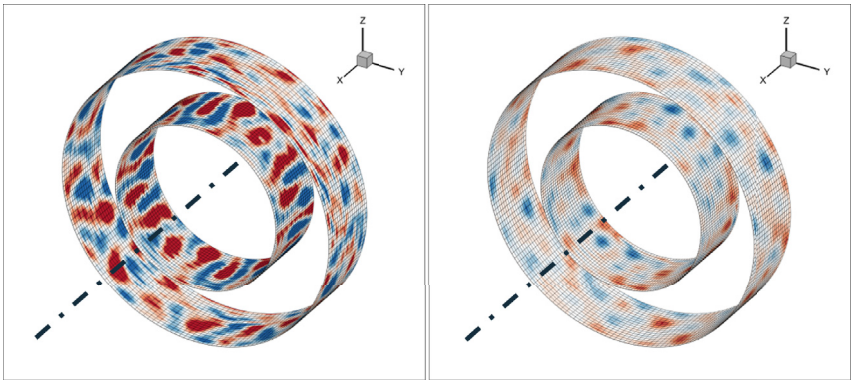

Fig. 18. Measured sound pressure distribution at a BPF on hub and shroud casing downstream of the TEC. Left: Hard wall TEC. Right: Lined TEC with same dynamic range.

power of the modes. It could be shown that the acoustic treatment results in a reduction of sound power ranging from 5 dB to 6 dB depending on the BPF component. Furthermore it could be determined which modes are attenuated most effectively. Detailed results are published in Ref. [37].

Submitted by Mirko Spitalny, Mirko.spitalny@dlr.de, German Aerospace Center (DLR), Germany, D. Broszat, I. Mahle, MTU Aero Engines AG, Germany, M. Bilson, F. Wallin, GKN Aerospace Engine Systems, Sweden.

6. Techniques and methods in aeroacoustics

6.1. A novel zonal approach for sound source prediction

Resolving the turbulent sound sources is computationally expensive and therefore many CAA methods rely on modelling the turbulent sound sources for the acoustic propagation. The vast number of different sound sources found in literature indicates that validation of these sound sources and improvements in modelling are necessary. In this contribution, we present a novel zonal RANS-LES method capable of fully resolving the sound sources in the area of interest [38]. It is denoted with “Overset” LES as a perturbation analysis of the compressible full Navier-Stokes equation is made over a background flow. With this novel approach, the turbulent sound sources can be studied directly.

An important aspect in the framework of all zonal methods is related to the proper seeding of inflow turbulence at upstream boundaries. For this purpose, 4D stochastic turbulence is generated with the help of the FRPM tool [39] and subsequently injected in the Overset-LES domain with the eddy-relaxation source term [38,40]. In Fig. 19, it is shown that the FRPM target and the actual vorticity distribution agree qualitatively very well. This eddy-relaxation source term is able to force the hydrodynamics while leaving the acoustics untouched, i.e., it is transparent for acoustic waves [41]. The application of the Overset-LES method to a NACA0012 trailing-edge was performed where mean flow and turbulence characteristics in the wake show a good agreement with experimental validation data [38]. In a subsequent step, the turbulent sound sources are coupled into a CAA simulation to perform the far-field acoustic propagation. Comparison of this far-field data with reference data illustrates that far-field acoustics are well captured (see Fig. 20).

Submitted by Paul Bernicke, p.bernicke@tu-braunschweig.de, and R.A.D. Akkermans, Institute of Fluid Mechanics, TU Braunschweig, Braunschweig, Germany.

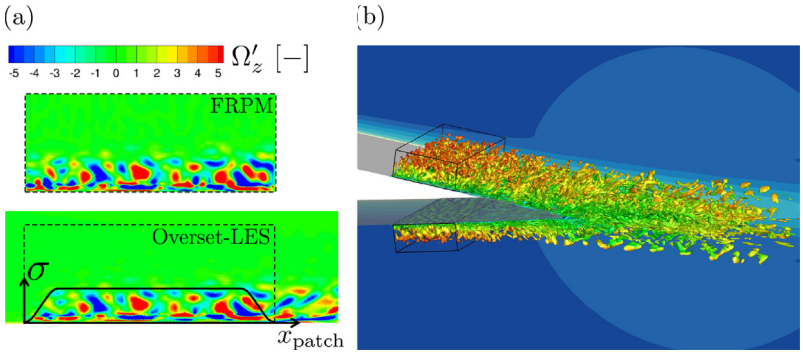

Fig. 19. (a) Instantaneous vertical vorticity distribution of the (top) FRPM target and (bottom) the actual distribution in Overset-LES. (b) Overset-LES simulation of NACA0012 trailing-edge region. Snapshot of turbulent structures visualised by the Q-criterion and coloured with the local Mach number.

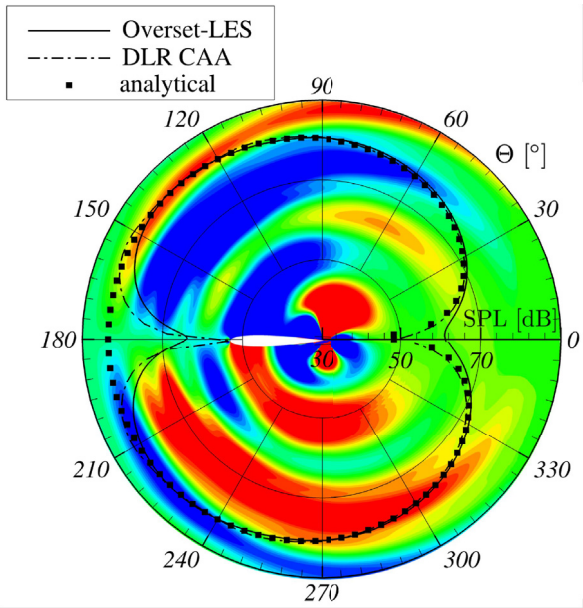

Fig. 20. Far-field OASPL directivity for NACA0012 trailing-edge noise, inset shows instantaneous pressure fluctuation contours resulting from the acoustic propagation of the Overset-LES sound sources.

6.2. Multi-level prediction concept for aircraft noise assessment

The strategic European paper "Flightpath 2050" claims dramatic reduction of noise for aviation transport scenarios. There is a consensus among experts that these far reaching objectives cannot be accomplished by application of noise reduction technologies at the level of aircraft components only. Step changes in aircraft technologies, aircraft configurations, and flight procedures are essential [42]. New aircraft concepts with entirely different propulsion concepts will emerge, including renewable energy sources, ranging from electric over hybrid to synthetic fuels. Within a joint research initiative of DLR, TU Braunschweig, and Empa, a multi-level, multi-fidelity approach is demonstrated in order to enable a comprehensive aircraft noise assessment [43], see Fig. 21. On level 1, high fidelity methods for predicting the aeroacoustic behavior of aircraft components (and installations) are required since in the early stages of the development of innovative noise reduction technology test data is not available [44]. The results are transferred to level 2, where radiation patterns of entire conventional and future aircraft concepts are assembled and noise emissions for single aircraft are computed. In level 3, large scale scenarios with many aircraft are considered to accurately predict the noise exposure for receivers on the ground [45]. Fig. 22 shows the noise benefit of an airframe noise reduction retrofit to an A320 aircraft vs. a replacement by a future a/c exploiting noise shielding in a yearly sound exposure level for a typical airport scenario. It is shown that reasonable predictions of the ground noise exposure level may be obtained, see Fig. 22.

Submitted by Jan Delfs, jan.delfs@dlr.de, L. Bertsch, DLR, Germany, C. Zellmann, Empa, Switzerland, L. Rossian, DLR, Germany, E.K. Far, T. Ring and S.C. Langer, TU Braunschweig, Germany.

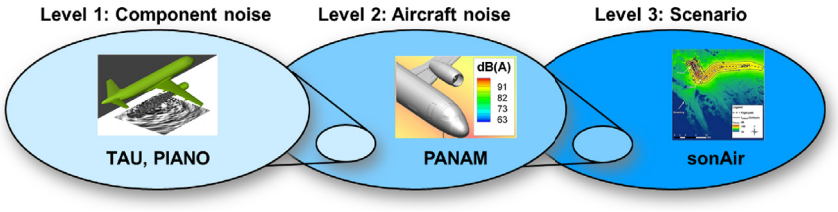

Fig. 21. Aircraft noise prediction chain based on DLR CFD/CAA codes TAU/PIANO, Parametric Aircraft Noise Analysis Module PANAM, and ground noise exposure level prediction sonAIR of EMPA.

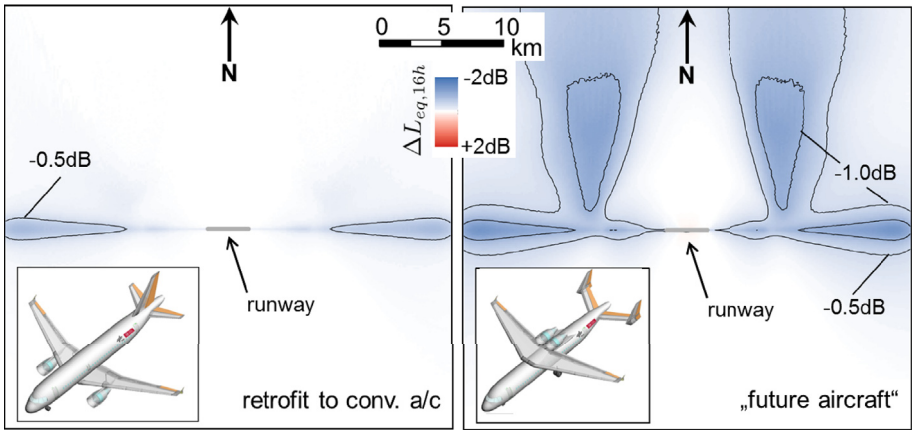

Fig. 22. Reduction of total noise exposure level (yearly, 6:00h-22:00h daily operation) for EMPA's SANC-TE airport scenario AP001S01 (see Ref. [43]) with a representative fleet mix, left: for airframe noise retrofit on A320, right: for replacement of A320 by future a/c concept (no departures to the south).

6.3. The modelling of the flow-induced vibrations of periodic flat and axial-symmetric structures using a wave finite element method

The vibrations induced by aeroacoustic fields exciting an elastic structure, arise strong interest in many engineering areas. The induced vibrations can damage internal devices and payloads, as in the case of a space-launcher lifting-off, or resulting in radiated noise, as in the case of transport means such as an aircraft fuselage, a train or vehicle cabin. Thus, the random vibrational and noise levels on the structures must be predicted before operating the system. However, the vibroacoustic analysis of structures under distributed stochastic excitation is often limited due to high computational costs, especially in the medium frequencies. The convective wavelength dependence requires the use of unaffordable meshes even for simple structures or low frequencies. On the other hand, the wave filtering properties and the ease in modelling the structural anisotropy, makes the periodic structures smart candidates for an enhancement of the vibroacoustic performances in many engineering areas. For these reasons, within the framework of homogeneous, periodic and axial-symmetric structures, a wave-based method is developed in order to overcome the state of the art, maintaining, at least, the same accuracy of the standard FE-based techniques [46,47]. A transfer matrix among the excited (wetted) and the response (target) points is built using a wave finite element method. The dynamics of the whole structure, for any boundary condition, damping model and curvature, is analysed through the dynamics of a single repetitive cell. A flexible link is created among the structural and the fluid meshes using the periodicity scale. In the case of homogeneous structures, such as laminated composite panels or cylinders, the computational cost is reduced by more than two orders of magnitude and the aliasing frequency is moved to higher frequencies, at the same time, as shown in Fig. 23. The method uses FE matrices extracted from any commercial code, thus has also the advantage of being able to use all the available FE formulations. The presence of complex structural parts which are not excited does not increase the size of the problem even if the stochastic response can be easily evaluated in such points. Differently, the standard FEM approaches would experience a strong increase in the number of degrees of freedom of the problem. Both a spatial, for flat structures, and an angular formulation, for axial-symmetric, curved and tapered structures, are developed and validated versus finite element and analytical models. The robustness of the technique is proved with uncorrelated and spatially-correlated loads, isotropic, laminates and complex structures [48]. A formulation including fluid inside the cabin has also been validated. Further ongoing developments are connected to the calculation of the transmission loss of flat and curved panels and cylinders, for acoustic and boundary layer excitation, whenever is the cell complexity. The research is also moving toward a formulation for strongly coupled problems.

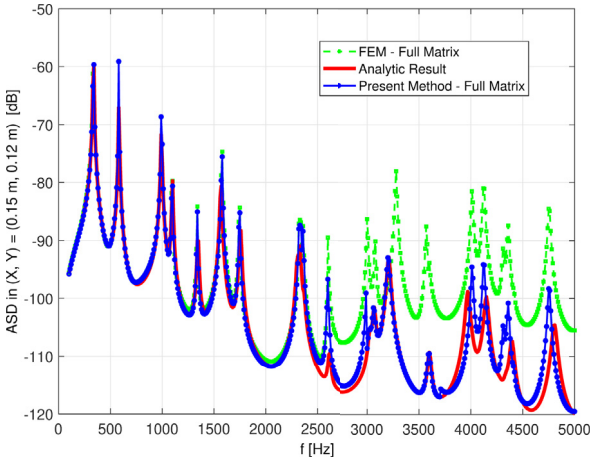

Fig. 23. Analytical-Numerical comparison for the nodal mobility auto spectral density (ASD). Simply Supported flat panel, under turbulent boundary layer excitation.

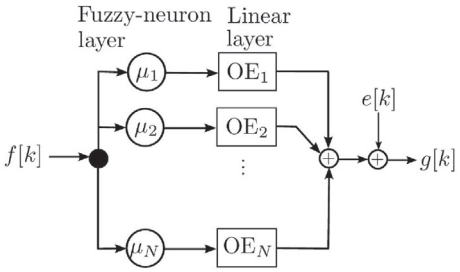

Fig. 24. Block diagram of the nonlinear model consisting of a neural network of linear sub-models (of Output-Error (OE) type) reproduced from Ref. [50].

Submitted by Fabrizio Errico, fabrizio.errico@ec-lyon.fr, Sergio De Rosa, Francesco Franco, Pasta-Lab, Dipartimento di Ingegneria Industriale Sezione Aerospaziale, Università degli Studi di Napoli "Federico II", Italy, Mohamed Ichchou, Olivier Bareille, Laboratoire de Tribologie et Dynamique des Systems (LTDS), Ecole Centrale de Lyon, France.

6.4. Nonlinear characterization of acoustic resonators based on neural networks

Combustion systems, such as gas turbines or rocket engines, may suffer from so-called thermoacoustic instabilities. Acoustic damping systems, like Helmholtz resonators or quarter wavelength cavities, are commonly used to control these instabilities [49]. Depending on the level of acoustical excitation, the damping induced by these devices differs significantly and thus behaves in a nonlinear manner mainly due to flow separation for high SPL. As shown in Ref. [49], accurate nonlinear models for all processes formulated in the time domain are mandatory to predict the resulting amplitudes for linearly unstable working conditions.

The nonlinear acoustic behavior of Helmholtz resonators is characterised by a data-based reduced-order modelling in Ref. [50]. This is done by a combination of high-resolution CFD simulation and system identification. This approach was followed in the linear regime in Ref. [51] and is now extended into the nonlinear regime [50]. For that purpose, a neural network consisting of parallel linear sub-models is proposed, as sketched in Fig. 24. This network is trained with data of a single CFD simulation. In this simulation, the resonator is acoustically excited by a broadband signal including the whole frequency and SPL range of interest. Within that range, a trained model can now describe the nonlinear acoustic behavior precisely. Fig. 25 depicts the reflection coefficient in dependency on the SPL for a trained model exemplary. For several test configurations, the trained network models show good agreement with experimental data. Such a model may serve as a nonlinear boundary condition in CFD or CAA simulations of complex systems.

Submitted by Kilian Förner, foerner@tfd.mw.tum.de, and Wolfgang Polifke, Technische Universität München, Germany.

6.5. Non-intrusive measurement of the correlation between the turbulent density and the radiated acoustic pressure in jets

Time-resolved and non-intrusive density measurements in compressible flows have been performed using a new Rayleigh scattering system developed at Ecole Centrale de Lyon. This optical measurement [52] is based on the linear relationship

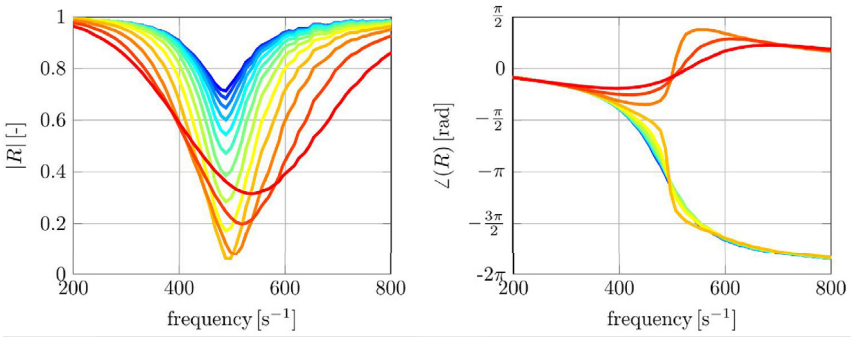

Fig. 25. Reflection coefficient described by a train network ranging form 80 dB (bluish) in 5 dB step up to 140 dB (reddish) reproduced from Ref. [50].

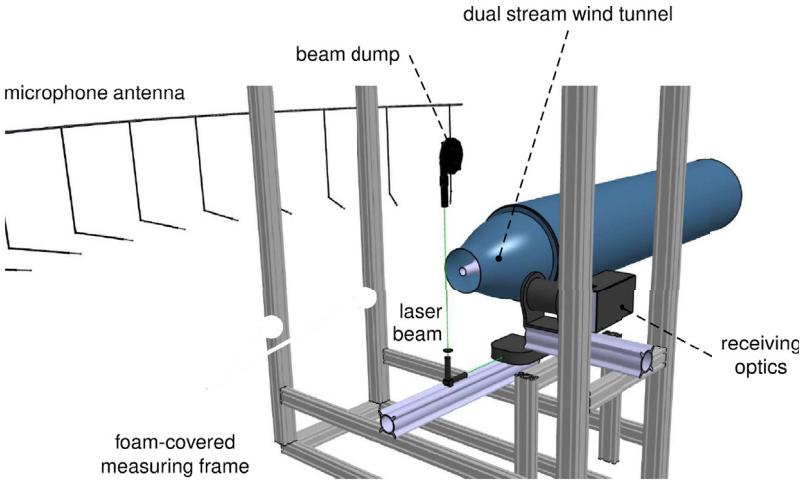

Fig. 26. Experimental set-up in the large anechoic wind tunnel of ECL, combining the Rayleigh scattering system and the microphone antenna in the acoustic far-field.

between the local density of the flow and the light power scattered by the molecules contained in the gas flow. This light power is here estimated through photon counting using a single photomultiplier [53], together with a high-frequency digitizer and a dedicated data processing scheme to determine a posteriori the photon flux. The effects of shot-noise and of a limited time-resolution, two well-known difficulties encountered by classical counters, have been reduced by the present method.

The optical system has been set-up in the anechoic environment of the dual-stream wind tunnel. Rayleigh scattering measurements have been coupled with far-field microphone acquisitions [54], see Fig. 26, in order to investigate noise production mechanisms in a high-Reynolds-number jet at Mach 0.9. The use of conditional statistics is better suited to examine the intermittent feature of jet turbulence and its associated noise. In this study, they are performed on density signals, and are based on the detection of high amplitude events in the acoustic pressure signal. The time delay associated with the acoustic propagation, around 5 ms, is taken into account to properly isolate the portions of the density signal. The result is displayed in Fig. 27 for a microphone located at 30° with respect to the jet axis in the downstream direction. Positive pressure peaks are considered and the conditional average is provided for six axial positions z/D, and for three radial positions y/D. The crosses indicate the point corresponding to the acoustic time delay for reaching the microphone. The identification of marked density variations may be observed near the end of jet potential core in the shear layer, and then closer to the jet axis further downstream.

Submitted by Bertrand Mercier, bertrand.mercier@ec-lyon.fr, Christophe Bailly, Université Lyon, Ecole Centrale de Lyon and LMFA UMR CNRS 5509, Ecully, France, Thomas Castelain, Université Lyon 1 and LMFA UMR CNRS 5509, Ecully, France.

6.6. Eigen Analysis in General Curvilinear Coordinates for prediction of noise propagation in aeroengine inlets

A new eigen analysis method (Eigen Analysis in General Curvilinear Coordinates, EAGCC) has been developed and applied to the prediction of linear acoustic propagation in an aeroengine inlet [55]. This method extends the state-of-the-art in eigen based acoustic prediction methods in that no simplifying assumptions/approximations are required with respect to duct geometry and mean flow other than that they are smoothly varying. The new analysis method is demonstrated on a representative model-

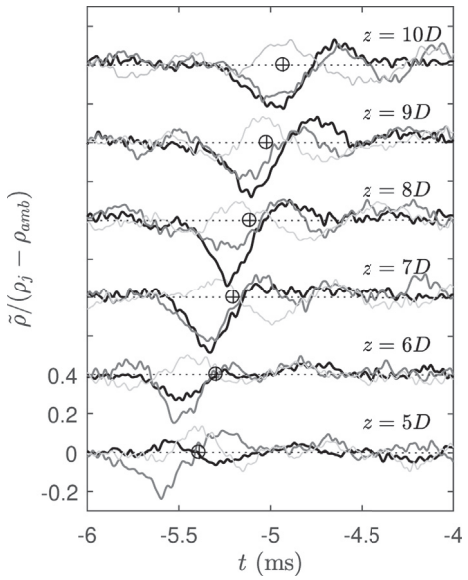

Fig. 27. Conditional averaging of density signals triggered by positive pressure peaks of a given microphone, and for six axial positions z/D. In dark, radial position y/D = 0 in gray, y/D = 0.25 and in lightgray, y/D = 0.5.

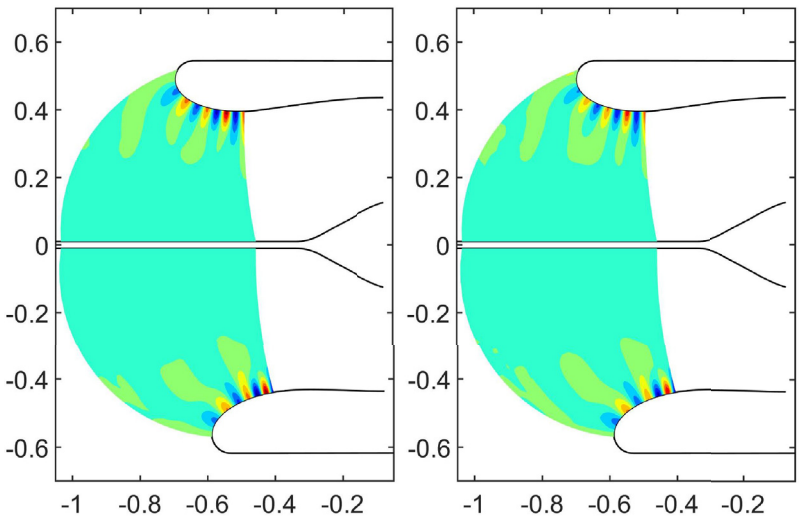

Fig. 28. Real part of static pressure at first blade passing frequency (left: EAGCC Solution, right: reference CFD Solution, both reproduced from Ref. [55]).

scale non-axisymmetric hardwall aeroengine inlet with non-uniform mean flow, and the results compared (Fig. 28) with a previously published 3D finite volume unsteady RANS CFD calculation [56]. The EAGCC results were quantitatively similar to those from the high fidelity CFD calculation, especially at first blade passing frequency (Fig. 29), but at much lower computational cost. The EAGCC method is therefore a promising route for design optimization. [55] also provides a brief summary of further developments needed to enable the method to be used in an industrial setting.

Submitted by Alexander Wilson, a.g.wilson@soton.ac.uk, Institute of Sound and Vibration Research, University of Southampton, United Kingdom.

7. Further aeroacoustic applications

7.1. System noise assessment of a tube-and-wing aircraft with geared turbofan engines

Geared turbofan engine concepts (GTF) with increased bypass ratios promise a reduction in specific fuel consumption. Furthermore, decreased noise generation due to reduced fan rotational speeds and jet exhaust velocities is predicted. Consequently,

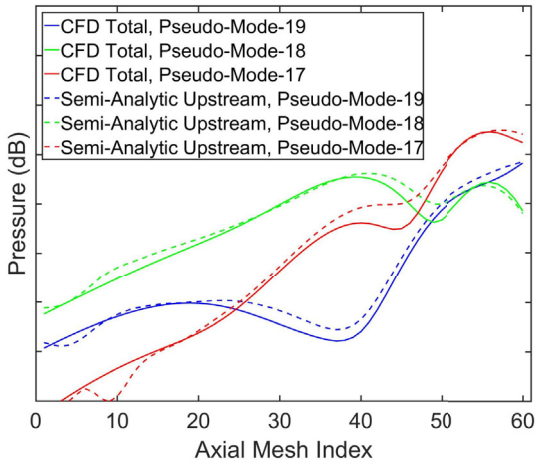

Fig. 29. Comparison of EAGCC and reference solution: Static pressure amplitude at first blade passing frequency near the outer wall in pseudo-circumferential harmonics 17 to 19 (reproduced from Ref. [55]).

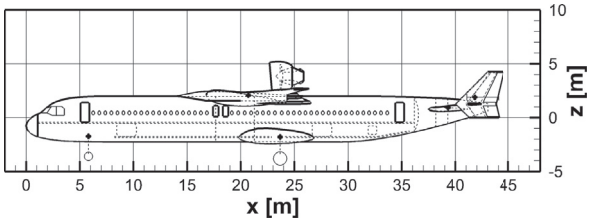

Fig. 30. Low-noise aircraft design "fanex".

the relevance of all remaining noise sources on board, e.g., the airframe contribution, is increased. A system noise assessment is required in order to identify the resulting noise source ranking and the overall noise impact as received on the ground. Therefore, a novel DLR and TU Braunschweig simulation process for aircraft design synthesis with integrated noise prediction capabilities is applied [42]. This process is upgraded in order to process external data from high-fidelity computation and measurements. Dedicated engine simulation data for a GTF engine [57] and experimental findings for selected high-lift systems [58] are incorporated into the study. Aircraft performance, e.g., direct operating costs, can now directly be compared to the predicted ground noise levels for different aircraft/engine combinations under consideration. The geared turbofan engine has been simulated on board of conventional tube-and-wing aircraft as well as on board of dedicated low-noise vehicles. It is demonstrated, that the combination of noise shielding and the geared turbofan concept is most effective. The most promising low-noise vehicle of the study (Fig. 30) is equipped with GTF engines that are shielded by the fuselage and the main wing. Consequently, the influence of the airframe noise sources is increased for this vehicle and any modification in order to reduce the airframe noise becomes especially effective. The application of low-noise airframe technologies to this vehicle reduces the overall aircraft noise as received on the ground. The isocontour areas are significantly smaller for this low-noise vehicle compared to the reference areas as depicted in Fig. 31 and described in Ref. [59].

Submitted by Lothar Bertsch, lothar.bertsch@dlr.de, F. Wolters, DLR, Germany, W. Heinze, TU Braunschweig, Germany, M. Pott-Pollenske and J. Blinstrub, DLR, Germany.

7.2. Helicopter noise footprint prediction in unsteady maneuvers

Different methodologies for the evaluation of the acoustic disturbance emitted by helicopter's main rotors during unsteady maneuvers have been investigated [60]. Nowadays, the simulation of noise emitted by helicopters is of great interest to designers, both for the assessment of the acoustic impact of helicopter flight on communities and for the identification of optimal-noise trajectories. Typically, the numerical predictions consist of the atmospheric propagation of a near-field noise model, extracted from an appropriate database determined through steady-state flight simulations/measurements (quasi-steady approach) [60]. In this work, three techniques for maneuvering helicopter noise predictions are compared: one considers a fully unsteady solution process, whereas the others are based on quasi-steady approaches. These methods are based on a three-step solution procedure: first, the main rotor's aeroelastic response is evaluated by a nonlinear beam-like rotor blade model coupled with a boundary element method for potential flow aerodynamics then, the aeroacoustic near field is evaluated through the

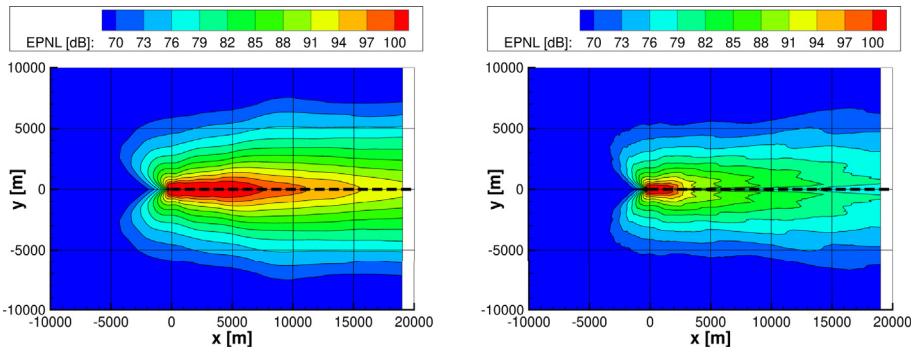

Fig. 31. Simulated EPNL isocontour areas along departure for the reference aircraft (left) and the low-noise "fanex" design (right).

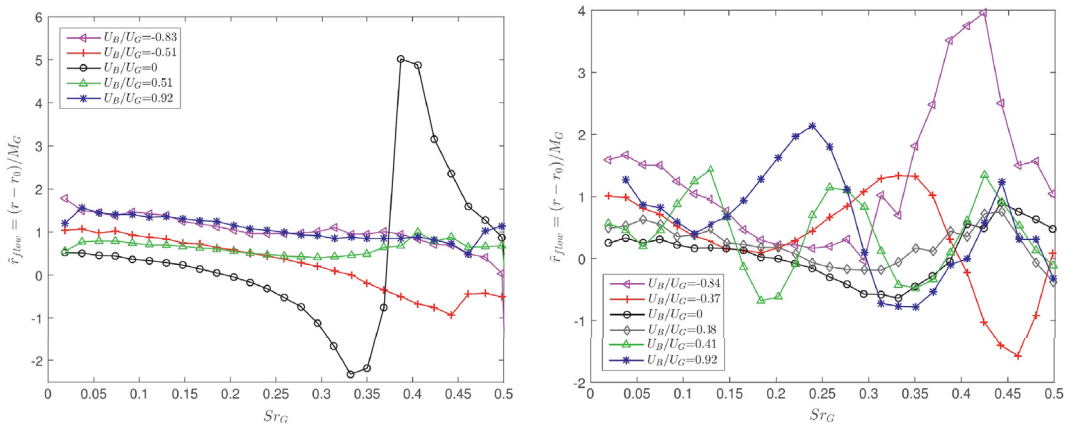

Fig. 32. Dimensionless real part of the impedance of a perforation with up and downstream sharp edges (27°, left), and with orthogonal edges (right), both under grazing flow of 16.8 m/s.

1A Farassat formulation, and finally, the noise is propagated to the ground by a ray tracing model [61]. Only the main rotor component is examined, although tail rotor contribution might be included as well. The numerical investigation examines the differences among the noise predictions provided by the three techniques, focusing on the assessment of the reliability of the results obtained through the two quasi-steady approaches as compared with those from the fully unsteady aeroacoustic solver [62].

Submitted by Massimo Gennaretti, m.gennaretti@uniroma3.it, Roma Tre University, Italy.

7.3. Strouhal number dependency of wall perforation impedance

In Ref. [63], the influence of low Mach number grazing-bias flow on the linear acoustic response of slit shaped wall perforations is determined in terms of a dimensionless acoustical impedance for Strouhal numbers $Sr_G = Wf/U_G$ of order unity, based on the perforation width W (in the flow direction), the frequency f and the grazing flow velocity U_G. The perforation is placed in the end-wall of an impedance tube. Results are provided in Fig. 32. in terms of the real part of the dimensionless impedance $r = \frac{1+R}{1-R}\left(\frac{Lh}{S}\right)$, where r_0 is the value of r in the absence of flow, c is the speed of sound, R is the reflection coefficient in the impedance tube of cross section S. (L h) is the minimum cross section of the slit [64]. Please note that in Ref. [63] there is a factor (L h/S) missing in the definition of r. The influence of edge geometries is studied. In particular, next to the classical geometry with sharp orthogonal edges, slanted slits under an angle of 30° with respect to the grazing flow direction are considered. Sound production, i.e. whistling potentiality corresponding to a negative real part of the real part of the impedance, is observed for various geometries and flow conditions. For combined bias/grazing flow, most of the oscillations in the impedance as a function of the Strouhal number are related to the limit behaviours of pure grazing and pure bias flows. A configuration with thin sharp edges (angle of 27°) both upstream and downstream corresponds to the geometry commonly used in theoretical models assuming an infinite thin wall. This configuration displays a behavior shown in Fig. 32(left), which is drastically different from the more common perforation geometries, such as the perforation with sharp orthogonal edges shown in Fig. 32(right).

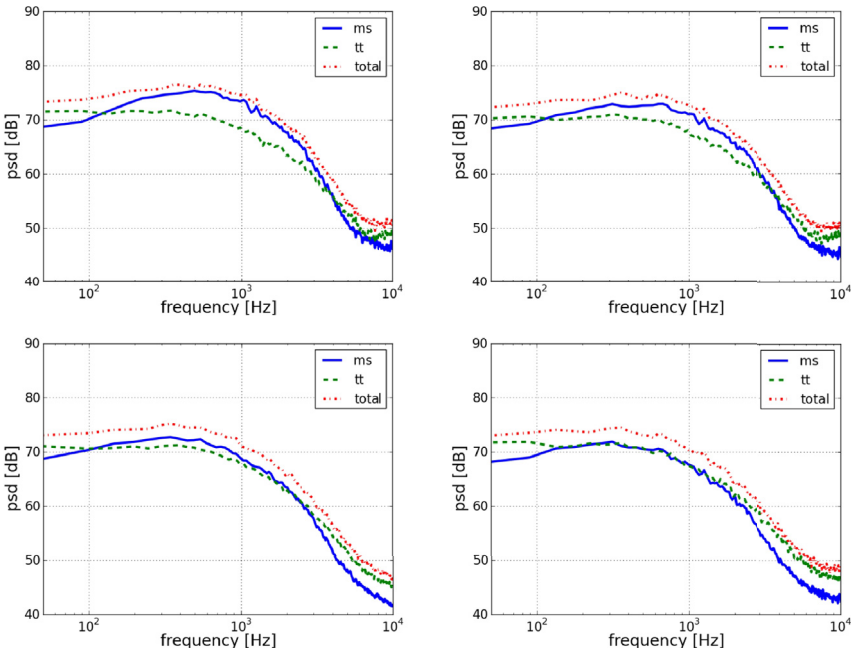

Fig. 33. Wall pressure spectra: (top left) isotropic turbulence approach, (top right) anisotropy of Reynolds stress tensors, (bottom left) anisotropy of Reynolds stress tensors with a length scale anisotropy stretching factor of 1.5, (bottom right) anisotropy of Reynolds stress tensors with a length scale anisotropy stretching factor of 2.

Submitted by Avraham Hirschberg, A.Hirschberg@tue.nl, Technische Universiteit Eindhoven, Eindhoven, The Netherlands.

7.4. Simulation of wall pressure fluctuations with synthetic anisotropic turbulence

The prediction of the high Reynolds number turbulent boundary layer wall pressure spectrum is important for the estimation and reduction of its impact on aircraft cabin noise level. Flat plate turbulent boundary layers are simulated using synthetic anisotropic turbulence generated by the fast random particle-mesh method [65,66]. The anisotropy is taken into account in two different stages. The first one considers the one-point statistics of the Reynolds stress tensor and the second additionally realizes anisotropic turbulence length scales. The impact of the turbulence structure on the resulting wall pressure spectra is studied. To determine spectra of wall pressure fluctuations, a Poisson equation is solved with unsteady right-hand side source terms derived from the synthetic turbulence realization. The contributions to wall pressure fluctuations from the mean-shear (ms) turbulence interaction term and the turbulence-turbulence (tt) interaction term are studied separately. The results show that contributions from both source terms have the same order of magnitude if turbulence anisotropy is considered, see Fig. 33. The result with anisotropic Reynolds stress tensors and a length scale stretching factor of 1.5 (turbulence length scale ratio between the streamwise and spanwise directions) is mostly consistent with the direct numerical simulation results from Kim [67]. Also good agreement for the correlation characteristics of the wall pressure field is found between the present results and databases from other investigators. Results of the spatial correlation shown in Fig. 34 represent similar contour shapes between the mean-shear term and the total result. In contrast, the turbulence-turbulence term exhibits isotropic correlation characteristics. From Fig. 35, it illustrates that the coherence from the turbulence-turbulence term decays much faster than the mean-shear term over the distance in both streamwise and spanwise directions.

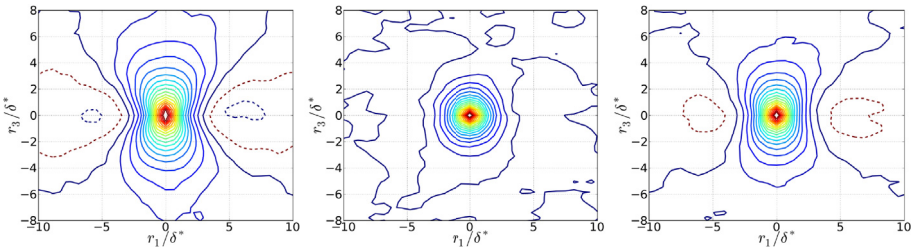

Fig. 34. Contour plots of spatial correlation (-), iso-contours, 0 to 0.9 with increment of 0.05 (- -), iso-contours, −0.05 and −0.1 (left) mean-shear (ms) contribution to $R_{pp}(r_1, r_3, 0)$ (middle) turbulence-turbulence (tt) contribution to $R_{pp}(r_1, r_3, 0)$ (right) combined (total) contribution to $R_{pp}(r_1, r_3, 0)$.

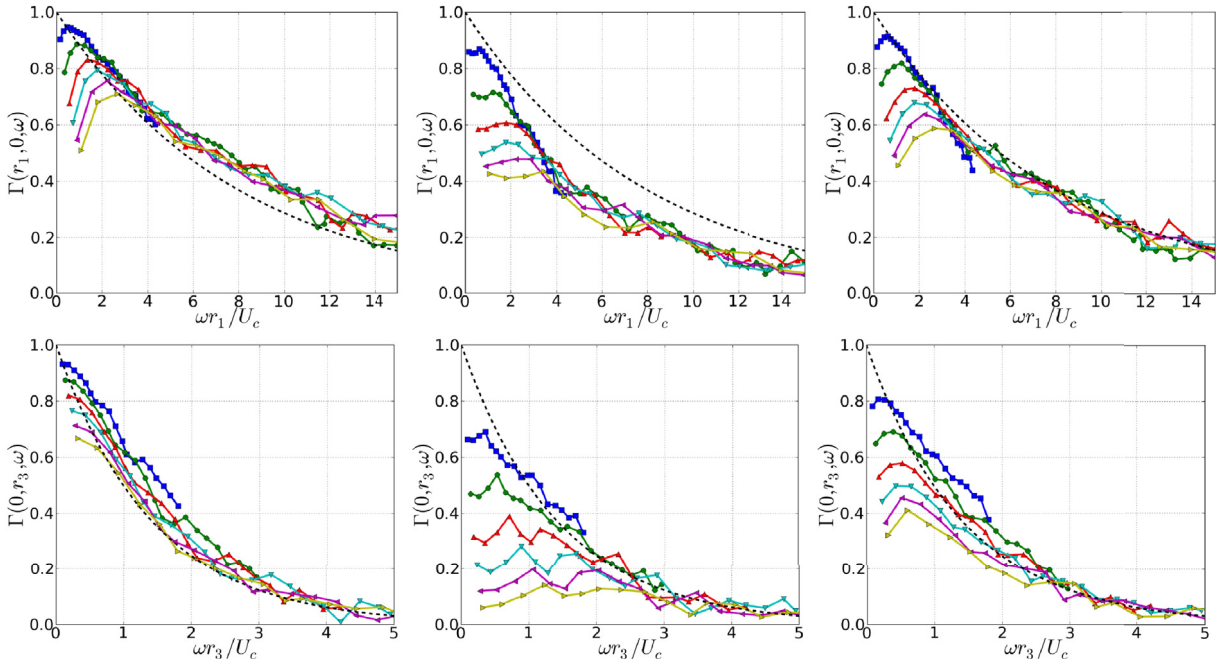

Fig. 35. Above: Streamwise coherence as a function of $\omega r_1/U_c$ for fixed space increments, $r_1 = 1.36delta^* - 8.18delta^*$ with increment of $1.36delta^*$ (- -), $\exp(-\alpha\omega r_1/U_c)$ with $\alpha = 0.125$ (left) coherence for p_{ms} (middle) coherence for p_{tt} (right) coherence for p_{total}. **Below:** Spanwise coherence as a function of $\omega r_3/U_c$ for fixed space increments, $r_3 = 0.78delta^* - 2.73delta^*$ with increment of $0.39delta^*$ (- -), $\exp(-\beta\omega r_3/U_c)$ with $\beta = 0.7$ (left) coherence for p_{ms} (middle) coherence for p_{tt} (right) coherence for p_{total}.

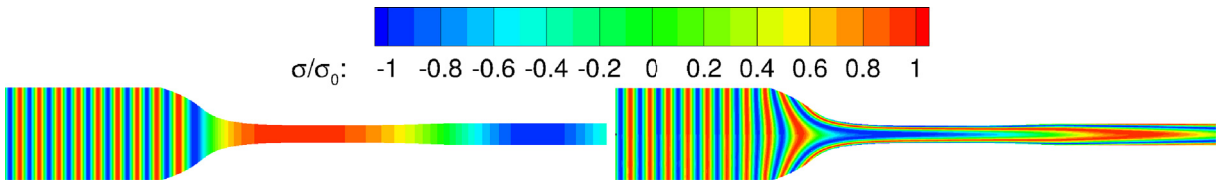

Fig. 36. Entropy fluctuation inside the nozzle. Left: quasi-1D model right: 2D model.

Submitted by Nan Hu, nan.hu@dlr.de, Nils Reiche and Roland Ewert, German Aerospace Center (DLR), Germany.

7.5. A model for indirect combustion noise generation with entropy shear dispersion

Indirect combustion noise is produced when perturbations such as entropy (temperature) spots are accelerated through a nozzle or a turbine stage. Entropy noise is classically modelled using quasi-1D models, where all perturbations are considered to be planar. This assumption is too restrictive for entropy waves at large frequencies and has been relaxed by Zheng et al. [68] who derived a 2D model taking into account the deformation of the entropy fluctuations. These fluctuations are reconstructed analytically using a 2D mean-flow field. The effect of the shear dispersion on the entropy waves is illustrated in Fig. 37. The model assumes linear perturbations and a harmonic regime, radial acoustic modes are considered to be cut-off for the frequencies of interest and vorticity is neglected so that pressure and velocity fluctuations are purely 1D and of acoustic nature. With these assumptions, entropy fluctuations appear as source terms in the mass and axial momentum equations averaged over the section, that are spatially discretized for numerical resolution. A thorough validation of this model has been performed by Emmanuelli et al. [69] using high-order CAA simulations and a Euler mean flow field. First, these simulations validate the analytical shear dispersion predicted by the model in Fig. 36. Second, they provide reference results for the entropy-generated noise. Numerical and modelled entropy-generated noise levels are visible in Fig. 37, where entropy-generated noise in the section downstream of the nozzle is represented as a function of the frequency in the form of thermoacoustic transfer functions. These results illustrate the accuracy of the model to predict entropy-generated noise through a subsonic nozzle. Comparisons with existing quasi-1D models highlight the overestimation of the predicted noise by these models as frequency rises because they fail to capture the decorrelation of the entropy noise sources inside the nozzle caused by the shear dispersion.

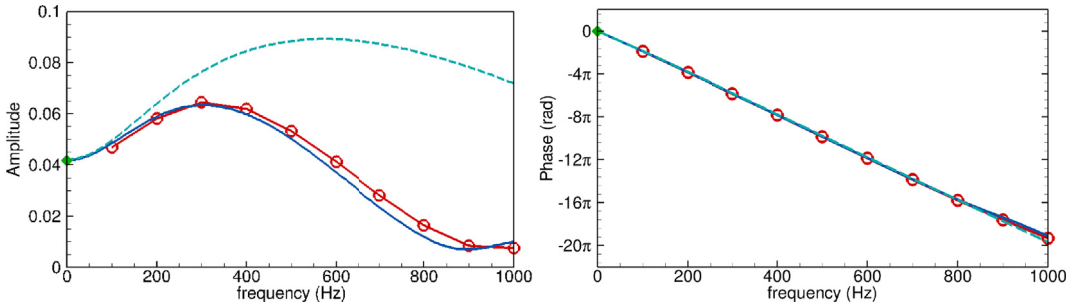

Fig. 37. Thermoacoustic transfer functions downstream of the nozzle. Left: amplitude, right: phase. Diamonds: compact solution, dashed line: quasi-1D model, straight line: 2D model, circles: CAA.

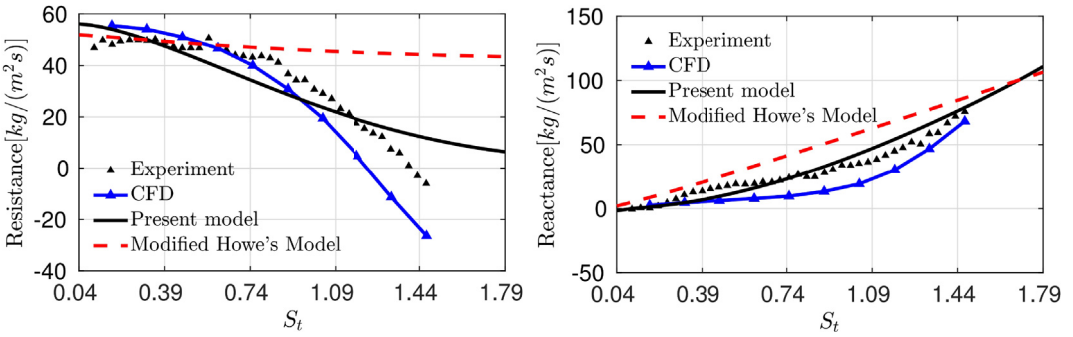

Fig. 38. The impedance (resistance on the left and reactance on the right) of a hole against Strouhal number. The hole length-to-diameter ratio is 0.5 and its mean flow Mach number is 0.062. Experimental and CFD results are from Ref. [71] at a Reynolds number of 16,000. The modified Howe results are based on [70].

Submitted by Maxime Huet, maxime.huet@onera.fr, A. Emmanuelli, T. Le Garrec, ONERA, S. Ducruix, Laboratoire EM2C, CNRS and CentraleSupélec, Université Paris-Saclay, France.

7.6. Acoustic modelling of holes and Helmholtz resonators

When acoustic waves are incident on a hole with mean flow passing through it, the acoustic energy is altered. This situation has wide practical relevance, from Helmholtz resonators and perforated liners used as dampers in aero-engines, power gas turbines and household appliances, to fuel injectors, to air from the lungs passing through the glottis. Two modelling assumptions can be made. The first is that the effect of viscosity is small except at the hole inlet edge, where flow separation generates vorticity. The second is that the mean flow sufficiently extends the linear regime, allowing for linear modelling even at quite large acoustic amplitudes. Typical models for the acoustics of short holes are derived from Howe's work [70], which captures the acoustic-to-vortical energy transfer. Such approaches have recently been shown to be unable to capture effects found in experiments in which holes are able to generate, as well as dissipate, acoustic energy in some low frequency regimes [71]. We have developed a modelling approach, which is new in accounting for two-way acoustic-vorticity coupling [72,73]. It is based on a Green's function method, applied to the geometry encompassing the hole and upstream and downstream regions. The Kutta condition is applied at the hole inlet edge, with the subsequent path of the shed vorticity prescribed, its shape being very important. Our predictions better match experimental results (see Fig. 38), and can capture the low frequency region in which holes can generate or damp acoustic energy [72]. We have used this approach to improve Helmholtz resonator models, by accounting for neck length and opening confinement [73]. We have, separately, developed the first acoustic models for Helmholtz resonators whose volume is at a different temperature to the device they are attached to - very often the case in for aero-engines and gas turbines [74]. The work received funding from the Chinese Scholarship Council and the ERC Starting Grant ACOULOMODE.

Submitted by Aimee S. Morgans, a.morgans@imperial.ac.uk, and D. Yang, Department of Mechanical Engineering, Imperial College London, United Kingdom.

7.7. Uncertainty assessment of a parametric aircraft system noise prediction

Parametric noise prediction in the context of aircraft design and flight procedure optimization has been around for more than 15 years. Continuous improvement of the models and the interconnection to other simulation tools allow today's mod-

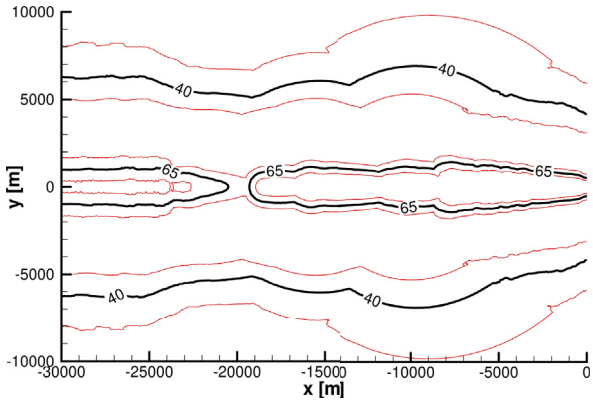

Fig. 39. Influence of uncertainty on predicted isocontour areas.

els to capture the major noise sources and relevant interactions along arbitrary flights [42]. Yet, reliable and comprehensive uncertainty analysis has not been available for these tools in the past. A new approach to assess uncertainties associated with the predicted noise levels was introduced in Refs. [75,76]. The overall uncertainty is thereby comprised of input data, noise modelling, and sound propagation uncertainties [77]. Obviously, each modelled noise source is associated with different input data and modelling uncertainties. According to the constantly changing noise source ranking along typical flight procedures, the overall uncertainty of the predicted ground noise level is highly variable. The new approach is applied to a DLR simulation process to establish a quality assessment and enable a reliable system noise prediction. It is demonstrated how the prediction results are affected by the underlying and prevailing uncertainty. Noise isocontour areas are subject to a significant change if the predictions are associated with their inherent uncertainty. Fig. 39 shows the impact on the predicted isocontour areas along a simulated approach. Uncertainty analysis reveals that uncertainty associated with input data and propagation effects can exceed the uncertainties of the noise source models when simulating conventional vehicles. Often, the focus of a quality assessment of prediction results is limited to the modelling of the noise source emission which is obviously not sufficient. The established

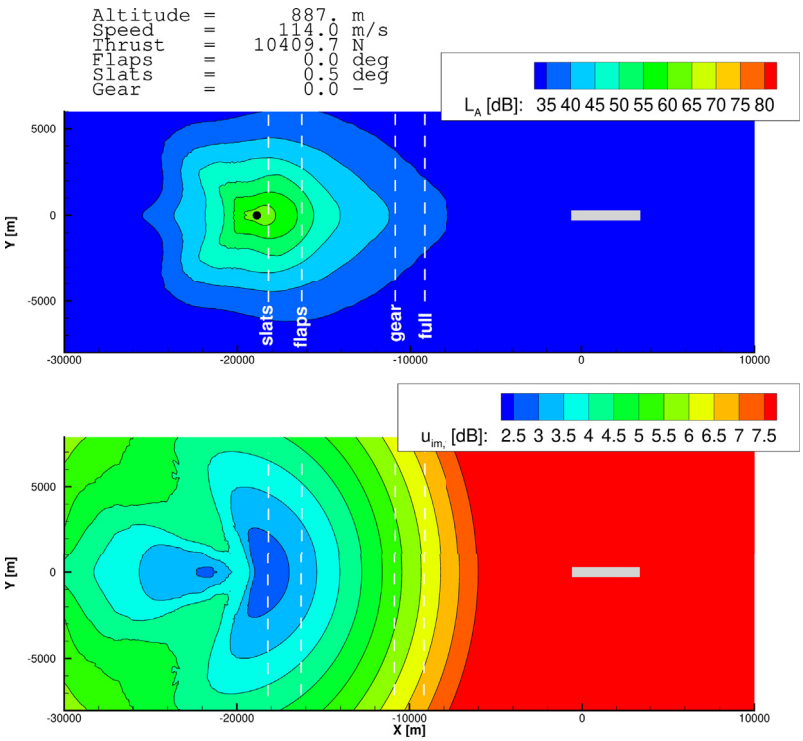

Fig. 40. Predicted noise immission and uncertainties for one arbitrary time step along approach flight.

uncertainty assessment can readily by applied to conventional tube-and-wing vehicles with turbofan engines [77]. Fig. 40 shows the predicted ground levels and the uncertainty for one simulation time step along an approach procedure.

Submitted by Beat Schäffer, Beat.Schaeffer@empa.ch, Empa, Switzerland, L. Bertsch, DLR, Germany, and S. Guérin, DLR, Germany.

References

[1] S. Guérin, A. Holewa, Fan tonal noise from aircraft aeroengines with short intake: a study at approach, Int. J. Aeroacoustics 12 (6) (2018), https://doi.org/10.1177/1475472X18789001. 1475472X1878900 http://journals.sagepub.com/doi/10.1177/1475472X18789001.

[2] F. Avallone, D. Casalino, D. Ragni, Impingement of a propeller-slipstream on a leading edge with a flow-permeable insert: a computational aeroacoustic study, Int. J. Aeroacoustics 12 (6) (2018), https://doi.org/10.1177/1475472X18788961. 1475472X1878896 http://journals.sagepub.com/doi/10.1177/1475472X18788961.

[3] G. Grasso, S. Moreau, J. Christophe, C. Schram, Multi-disciplinary optimization of a contra-rotating fan, Int. J. Aeroacoustics 12 (6) (2018), https://doi.org/10.1177/1475472X18789000. 1475472X1878900 http://journals.sagepub.com/doi/10.1177/1475472X18789000.

[4] J. Kennedy, P. Eret, G.J. Bennett, A parametric study of airframe effects on the noise emission from installed contra-rotating open rotors, Int. J. Aeroacoustics 12 (6) (2018), https://doi.org/10.1177/1475472X18789003. 1475472X1878900 http://journals.sagepub.com/doi/10.1177/1475472X18789003.

[5] S. Moreau, M. Roger, Advanced noise modeling for future propulsion systems, Int. J. Aeroacoustics 12 (6) (2018), https://doi.org/10.1177/1475472X18789005. 1475472X1878900 http://journals.sagepub.com/doi/10.1177/1475472X18789005.

[6] C. Zellmann, B. Schäffer, J.M. Wunderli, U. Isermann, C.O. Paschereit, Aircraft noise emission model accounting for aircraft flight parameters, J. Aircr. 55 (2) (2018) 682–695, https://doi.org/10.2514/1.C034275.

[7] C. Zellmann, Development of an Aircraft Noise Emission Model Accounting for Flight Parameters. (Ph.D. Thesis), Institute of Fluid Dynamics and Technical Acoustics, Technische Universität Berlin, 2018 https://doi.org/10.14279/depositonce-6712.

[8] J.M. Wunderli, C. Zellmann, M. Köpfli, M. Habermacher, O. Schwab, F. Schlatter, B. Schäffer, sonAIR - a GIS-integrated spectral aircraft noise simulation tool for single flight prediction and noise mapping, Acta Acustica United Acustica 104 (3) (2018) 440–451, https://doi.org/10.3813/AAA.919180.

[9] O. Cetin, S.R. Koh, M. Meinke, W. Schröder, Numerical analysis of the impact of the interior nozzle geometry on low mach number jet acoustics, J. Flow, Turbul. Combust. 98 (2) (2017) 417–443.

[10] C. Bogey, C. Bailly, Influence of nozzle-exit boundary-layer conditions on the flow and acoustics fields of initially laminar jets, J. Fluid Mech. 63 (2010) 507–538.

[11] G.A. Brès, J.W. Nichols, S.K. Lele, F.E. Ham, Towards best practices for jet noise predictions with unstructured large eddy simulations, in: Proceedings: 42nd AIAA Fluid Dynamics Connference and Exhibit, 25 - 28 June 2012 https://doi.org/10.2514/6.2012-2965. New Orleans; AIAA Paper 2012-2965.

[12] M. Lorteau, F. Cléro, F. Vuillot, Analysis of noise radiation mechanisms in hot subsonic jet from a validated les solution, Phys. Fluids 27 (7) (2015) 075108.

[13] F. Vuillot, N. Lupoglazoff, M. Lorteau, F. Cléro, Large-eddy simulation of jet noise from unstructured grids with turbulent nozzle boundary layer, in: Proceedings: 22nd AIAA/CEAS Aeroacoustics Conference, 30 May - 01 June 2016 https://doi.org/10.2514/6.2016-3046. Lyon, France; AIAA-Paper 2016-3046.

[14] J.-B. Chapelier, M. de la Llave Plata, F. Renac, E. Lamballais, Evaluation of a high-order dg method for the dns of turbulent flows, Comput. Fluid 95 (2014) 210–226.

[15] F. Renac, M. de la Llave Plata, E. Martin, J.-B. Chapelier, V. Couaillier, aghora: a high-order dg solver for turbulent flow simulations, idihom: industrialisation of high-order methods “a top down approach.”, Notes Numer. Fluid Mech. Multidiscip. Design 128 (2015) 315–335.

[16] M. Lorteau, M. de la Llave Plata, V. Couaillier, Turbulent jet simulation using high-order dg methods for aeroacoustic analysis, Int. J. Heat Fluid Flow 70 (2018) 380–390.

[17] J.-B. Chapelier, M. de la Llave Plata, E. Lamballais, Development of a multiscale les model in the context of a modal discontinuous galerkin method, Comput. Methods Appl. Mech. Eng. 307 (2016) 275–299.

[18] V. Fleury, C. Bailly, E. Jondeau, M. Michard, D. Juvè, Space time correlations in two subsonic jets using dual particle image velocimetry measurements, AIAA J. 46 (2008) 2498–2509, https://doi.org/10.2514/1.35561.

[19] M. Mancinelli, T. Pagliaroli, R. Camussi, T. Castelain, On the hydrodynamic and acoustic nature of pressure proper orthogonal decomposition modes in the near field of a compressible jet, J. Fluid Mech. 836 (2018) 998–1008, https://doi.org/10.1017/jfm.2017.839.

[20] M. Mancinelli, T. Pagliaroli, A. Di Marco, R. Camussi, T. Castelain, O. Léon, Hydrodynamic and acoustic wavelet-based separation of the near-field pressure of a compressible jet, in: Proceedings: 22nd AIAA/CEAS Aeroacoustics Conference, 30 May - 01 June 2016 https://doi.org/10.2514/6.2016-2864. Lyon, France; AIAA Paper 2016-2861.

[21] M. Mancinelli, T. Pagliaroli, A. Di Marco, R. Camussi, T. Castelain, Wavelet decomposition of hydrodynamic and acoustic pressures in the near field of the jet, J. Fluid Mech. 813 (2017) 716–749, https://doi.org/10.1017/jfm.2016.869.

[22] J. Punekar, E.J. Avital, X. Li, Crackle: measurements and analysis of supersonic jet noise, J. Acoust. Soc. Am. 141 (6) (2017) EL567–EL573.

[23] M. Behn, L. Klähn, U. Tapken, Comprehensive experimental investigation of mode transmission through stator vane rows: results and calibration of an analytical prediction model, in: 23rd AIAA/CEAS Aeroacoustics Conference, 05-09 June 2017, Denver, Colorado (USA), AIAA 2017-3218.

[24] M. Behn, R. Kisler, U. Tapken, Efficient azimuthal mode analysis using compressed sensing, in: 22nd AIAA/CEAS Aeroacoustics Conference, 30 May-01 June 2016, Lyon, France, AIAA 2016-3038.

[25] M. Behn, U. Tapken, P. Puttkammer, R. Hagmeijer, N. Thouault, Comparative study of different analytical approaches for modelling the transmission of sound waves through turbomachinery stators, in: 22nd AIAA/CEAS Aeroacoustics Conference, 30 May-01 June 2016, Lyon, France, AIAA 2016-2927.

[26] S.N. Smith, Discrete Frequency Sound Generation in Axial Flow Turbomachines, Aeronautical Research Council Reports and Memoranda 3709, 1971.

[27] D. Casalino, A.F.P. Ribeiro, E. Fares, S. Noelting, Lattice-Boltzmann aeroacoustic analysis of the lagoon landing-gear configuration, AIAA J. 52 (6) (2014).

[28] D. Casalino, A.F.P. Ribeiro, E. Fares, Facing rim cavities fluctuation modes, J. Sound Vib. 333 (2014) 2812–2830.

[29] E. Fares, D. Casalino, M.R. Khorrami, Evaluation of airframe noise reduction concepts via simulations using a lattice Boltzmann approach, in: AIAA Paper 2015-2988, 2015.

[30] D. Casalino, A. Hazir, A. Mann, Turbofan broadband noise prediction using the lattice Boltzmann method, AIAA Paper 2015-2988 56 (2) (2018) 609–628, https://doi.org/10.2514/1.J055674.

[31] T.J. Cox, P. D'Antonio, Acoustic Absorbers and Diffusers, second ed., Taylor & Francis, Oxon, 2009, ISBN: 9781482266412, p. 496, https://doi.org/10.4324/9781482266412. eBook.

[32] E. Rivet, S. Karkar, H. Lissek, Broadband low-frequency electroacoustic absorbers through hybrid sensor-/shunt-based impedance control, IEEE Trans. Control Syst. Technol. 25 (1) (2017) 63–72.

[33] R. Boulandet, H. Lissek, S. Karkar, M. Collet, G. Matten, M. Ouisse, M. Versaevel, Duct modes damping through an adjustable electroacoustic liner under grazing incidence, J. Sound Vib. 426 (2018) 19–33.

[34] S. Narayanan, P. Chaitanya, S. Haeri, P. Joseph, J.W. Kim, C. Polacsek, Airfoil noise reductions through leading edge serrations, Phys. Fluids 27 (2) (2015), https://doi.org/10.1063/1.4907798.

[35] G. Reboul, A. Cader, C. Polacsek, T. Le Garrec, R. Barrier, N. Ben Nasr, Caa prediction of rotor-stator interaction using synthetic turbulence: application to a low-noise serrated ogv, in: Proceedings: 23rd AIAA/CEAS Aeroacoustics Conference, Denver (USA), 5 - 9 June 2017 https://doi.org/10.2514/6.2017-3714. AIAA Paper 2017-3714 2.

[36] U. Tapken, L. Enghardt, Optimization of sensor arrays for radial mode analysis in flow ducts, in: Proceedings of the AIAA/CEAS Aeroacoustics Conference (27th AIAA Aeroacoustics Conference),Cambridge, Massachusetts, USA, 08 May - 10 May 2006 https://doi.org/10.2514/6.2006-2638. AIAA Paper2006-2638.

[37] D. Broszat, I. Mahle, M. Billson, F. Wallin, M. Spitalny, Aerodynamic and acoustic testing of a turbine exhaust case with integrated hot stream liners in a realistic multi-stage environment, in: Proceedings of the 24th AIAA/CEAS Aeroacoustics Conference 2018, Atlanta, Georgia 1 of 7, 2018, pp. 3558–3569, https://doi.org/10.2514/6.2018-3916.
[38] R. Akkermans, P. Bernicke, R. Ewert, J. Dierke, Zonal overset-les with stochastic volume forcing, Int. J. Heat Fluid Flow 70 (2018) 336–347. https://doi.org/10.1016/j.ijheatfluidflow.2017.11.005, http://www.sciencedirect.com/science/article/pii/S0142727X1730379X.
[39] P. Bernicke, R. Akkermans, R. Ewert, J. Dierke, Overset les for trailing-edge noise computations, in: Proceedings of 23rd AIAA/CEAS Aeroacoustics Conference, Denver, USA, AIAA Paper 2017-3170, 2017 https://doi.org/10.2514/6.2017-3170.
[40] P. Bernicke, R. Akkermans, R. Ewert, J. Dierke, Overset les with an acoustic relaxation term for sound source simulations, in: Proceedings of 22th AIAA/CEAS Aeroacoustics Conference, Lyon, AIAA 2016-3031, June 2016 https://doi.org/10.2514/6.2016-3031.
[41] P. Bernicke, R. Akkermans, R. Ewert, J. Dierke, Overset les for trailing-edge noise computations, in: Proceedings of 23rd AIAA/CEAS Aeroacoustics Conference, Denver, AIAA 2017-3170, June 2017 https://doi.org/10.2514/6.2017-3170.
[42] L. Bertsch, W. Heinze, M. Lummer, Application of an aircraft design-to-noise simulation process, in: Proceedings of the 14th AIAA Aviation Technology, Integration, and Operations Conference, 2014 https://doi.org/10.2514/6.2014-2169.
[43] J. Delfs, L. Bertsch, C. Zellmann, L. Rossian, E. Kian Far, T. Ring, S. Langer, Aircraft noise assessment-from single components to large scenarios, Energies 11 (2) (2018) 429, https://doi.org/10.3390/en11020429 (2018).
[44] L. Rossian, R. Ewert, J. Delfs, Prediction of airfoil trailing edge noise reduction by application of complex porous material, in: New Results in Numerical and Experimental Fluid Mechanics XI, Springer, New York, NY, USA, 2018, pp. 647–657.
[45] C. Zellmann, B. Schäffer, J. Wunderli, U. Isermann, C.O. Paschereit, Aircraft noise emission model accounting for aircraft flight parameters, J. Aircr. 2017 (2017) 1–15.
[46] F. Errico, M. Ichchou, S. De Rosa, O. Bareille, F. Franco, A wfe and hybrid fe/wfe technique for the forced response of stiffened cylinders, Adv. Aircraft Spacecraft Sci. 5 (1) (2018) 1–19.
[47] F. Errico, M. Ichchou, S. De Rosa, O. Bareille, F. Franco, A wave finite element technique for the calculation of the flow-induced vibrations of periodic and axial-symmetric structures, in: 6th NOVEM Noise and Vibration Emerging Methods 7-9 May 2018, vol. 5, 2018, pp. 1–19 (1) novem2018.sciencesconf.org.
[48] F. Errico, M. Ichchou, S. De Rosa, O. Bareille, F. Franco, The modelling of the flow-induced vibrations of periodic flat and axial-symmetric structures with a wave-based method, J. Sound Vib. 424 (2018) 32–47, https://doi.org/10.1016/j.jsv.2018.03.012.
[49] K. Förner, A. Cárdenas Miranda, W. Polifke, Mapping the influence of acoustic resonators on rocket engine combustion stability, J. Propuls. Power 31 (4) (2015) 1159–1166.
[50] K. Förner, W. Polifke, Nonlinear aeroacoustic identification of helmholtz resonators based on a local-linear neuro-fuzzy network model, J. Sound Vib. 407 (2017) 170–190.
[51] K. Förner, W. Polifke, Aero-acoustic characterization of helmholtz resonators in the linear regime with system identification, in: 22nd International Congress on Sound and Vibration, Florence, Italy, 2015.
[52] J. Panda, R.G. Seasholtz, Experimental investigation of density fluctuations in high speed jets and correlation with generated noise, J. Fluid Mech. 450 (2002) 97–130.
[53] B. Mercier, T. Castelain, E. Jondeau, C. Bailly, Density fluctuations measurement by Rayleigh scattering using a single photomultiplier, AIAA J. 56 (4) (2018) 1310–1316.
[54] B. Mercier, T. Castelain, C. Bailly, Experimental investigation of the turbulent density - farfield sound correlations in compressible jet, Int. J. Aeroacoustics 17 (4–5) (2018) 521–540, https://doi.org/10.1177/1475472X18778274.
[55] A.G. Wilson, Eigen analysis in general curvilinear coordinates for prediction of noise propagation in aeroengine inlets, in: Presented at 23rd AIAA/CEAS Aeroacoustics Conference, Denver, Colorado, 5-9 June 2017, AIAA-2017-3704.
[56] M. Doherty, H. Namgoong, Impact of turbofan intake distortion on fan noise propagation and generation, in: Presented at 22nd AIAA/CEAS Aeroacoustics Conference, Lyon, May/June 2016, AIAA 2016-2841.
[57] J. Pott-Pollenske, M.J.W. Wild, L. Bertsch, Aerodynamic and acoustic design of silent leading edge device, in: 20th AIAA/CEAS Aeroacoustics Conference Proceedings, Atlanta, Georgia, USA, 16 - 20 June 2014 https://doi.org/10.2514/6.2014-2076.
[58] R. Becker, F. Wolters, M. Nauroz, T. Otten, Development of a Gas Tubine Performance Code and its Application to Preliminary Engine Design, Deutscher Luft- und Raumfahrtkongress, 2011. paper DLRK 2011-241485.
[59] L. Bertsch, F. Wolters, W. Heinze, M. Pott-Pollenske, J. Blinstrub, System noise assessment of a tube-and-wing aircraft with geared turbofan engines, in: Proceedings of the AIAA SciTech Forum, 2018 https://doi.org/10.2514/6.2018-0264.
[60] G. Bres, K. Brentner, G. Perez, et al., Maneuvering rotorcraft noise prediction, J. Sound Vib. 275 (2004) 719–738 (2004).
[61] L. Trainelli, M. Gennaretti, G. Bernardini, A. Rolando, C. Riboldi, M. Redaelli, L. Riviello, A. Scandroglio, Innovative helicopter in-flight noise monitoring systems enabled by rotor-state measurements, Noise Mapp. 3 (2016) 190–215, https://doi.org/10.1515/noise-2016-0014 (2016).
[62] M. Massimo Gennaretti, G. Bernardini, J. Serafini, A. Anobile, S. Hartjes, Helicopter noise footprint prediction in unsteady maneuvers, Int. J. Aeroacoustics 16 (3) (2017) 165–180, https://doi.org/10.1177/1475472X17709927.
[63] E. Moers, D. Tonon, A. Hirschberg, Strouhal number dependency of the aero-acoustic response of wall perforations under combined grazing-bias flow, J. Sound Vib. 389 (2017) 292–308.
[64] D. Tonon, E. Moers, A. Hirschberg, Quasi-steady acoustic response of wall perforations subject to a grazing-bias flow combination, J. Sound Vib. 332 (2013) 1654–1673.
[65] N. Hu, N. Reiche, R. Ewert, Simulation of turbulent boundary layer wall pressure fluctuations via Poisson equation and synthetic turbulence, J. Fluid Mech. 826 (2017) 421–454.
[66] R. Ewert, J. Dierke, J. Siebert, A. Neifeld, C. Appel, M. Siefert, O. Kornow, Caa broadband noise prediction for aeroacoustic design, J. Sound Vib. 330 (2011) 4139–4160.
[67] J. Kim, On the structure of pressure fluctuations in simulated turbulent channel flow, J. Fluid Mech. 205 (1989) 421–451.
[68] J. Zheng, M. Huet, F. Cléro, A. Giauque, S. Ducruix, A 2d-axisymmetric analytical model for the estimation of indirect combustion noise in nozzle flows, in: Proceedings of the 21st AIAA/CEAS Aeroacoustics Conference, Paper AIAA 2015-2974, 2015.
[69] A. Emmanuelli, M. Huet, T. Le Garrec, S. Ducruix, Caa study of entropy noise in nozzle flow for the validation of a 2d semi-analytical model, in: Proceedings of ASME Turbo Expo, 2017, Paper GT2017-63640.
[70] M.S. Howe, On the theory of unsteady high Reynolds number flow through a circular aperture, Proc. Roy. Soc. Lond. A 366 (1725) (1979) 205–223.
[71] J. Su, J. Rupp, A. Garmory, J.F. Carrotte, Measurements and computational fluid dynamics predictions of the acoustic impedance of orifices, J. Sound Vib. 352 (2015) 174–191.
[72] D. Yang, A.S. Morgans, A semi-analytical model for the acoustic impedance of finite length circular holes with mean flow, J. Sound Vib. 384 (2016) 294–311.
[73] D. Yang, A.S. Morgans, The acoustics of short circular holes opening to confined and unconfined spaces, J. Sound Vib. 393 (2017) 41–61.
[74] D. Yang, A.S. Morgans, Acoustic models for cooled helmholtz resonators, AIAA J. 55 (9) (2017) 3120–3127.
[75] B. Schäffer, S. Pluess, G. Thomann, Estimating the model-specific uncertainty of aircraft noise calculations, Appl. Acoust., Special Issue: Air Transp. Noise, ISSN: 0003-682X 84 (2014) 58–72.
[76] G. Thomann, Uncertainties of Measured and Calculated Aircraft Noise and Consequences in Relation to Noise Limits. (PhD Thesis), ETH Zürich, 2007. No. 17433.
[77] L. Bertsch, B. Schäffer, S. Guérin, Towards an uncertainty analysis for parametric aircraft system noise prediction, in: Proceedings 12th ICBEN Congress on Noise as a Public Health Problem, Zürich, Switzerland, 18 - 22 June 2017, Paper 0806-3937 (2017) 12.